

---

# *Phase-Shifting Interferometry*

---

## 1 Contents

---

### 1.1 Hyperlinks

### 1.2 Sections

Table of Contents...	1
Hyperlinks...	1.1
Sections...	1
Introduction...	2
Basic Concepts of PSI...	3
Two Beam Interference and 4-Step PSI Algorithm...	3.1
Define $a_0$ $a_1$ and $a_2$ ...	3.1
Two-beam interference equation...	3.1
TanPhase...	3.1
Four step phase equation...	3.1
Phase-shifting vs phase stepping...	3.2
Sinc...	3.2
Phase unwrapping...	3.3
Three-Step Algorithms...	4.1
Three-step algorithm example 1...	4.1.1
Three-step algorithm example 2...	4.1.2
Three-step algorithm example 3...	4.1.3
2+1 Algorithm (Angel and Wizinowich)...	4.1.4
Carre Algorithm...	4.2.0
Least Squares...	5
Four steps...	5.1
Synchronous Detection...	5.2
Five Step Algorithm...	5.3
Five steps (Schwider-Hariharan Algorithm)...	5.4
Weighted Coefficients - Improved Algorithms...	5.5
6 step algorithm...	5.5
7 step algorithm...	5.5
Errors...	6
Error due to incorrect phase-shift between data frames...	6.1
Four Steps Phase Shifting Error...	6.1.1
4 step phase error due to phase shift...	6.1.1

---

Three Steps Phase Shifting Error...	6.1.2
Five Steps Phase Shifting Error...	6.1.3
Schwider-Hariharan Phase Shifting Error...	6.1.4
Six Step Phase Shifting Error...	6.1.5
Seven Step Phase Shifting Error...	6.1.6
Error due to vibration...	6.2
Error due to detector non-linearity...	6.3
Four Steps detector nonlinearity error...	6.3.1
Three Steps detector nonlinearity error...	6.3.2
Five Steps detector nonlinearity error...	6.3.3
Schwider-Hariharan detector nonlinearity error...	6.3.4
Six Step detector nonlinearity error...	6.3.5
Seven Step detector nonlinearity error...	6.3.6
Error due to stray reflections...	6.4
Quantization error...	6.5
Frequency stability error...	6.6
Intensity fluctuations error...	6.7
Phase shifters...	7
Moving Mirror...	7.1
Moving Diffraction Grating...	7.2
AO Bragg Cell...	7.3
Rotating Half-Wave Plate...	7.4
Phase Shifter Calibration...	7.5
Phase-Shifting Interferometer...	7.6
Software modules...	8
Plot Phase Error Module...	8.1
Vibration Error Module...	8.2
Plot Vibration Error Module...	8.3
Phase unwrapping module...	8.4
References...	9

## 2 Introduction

---

Computers are changing nearly everything we do. Computers have made enormous improvements in interferometric metrology. While interferometry concepts are old, by combining old interferometry concepts with modern electronics, computers, and software, interferometry has become an exciting modern topic.

An interferogram contains an enormous amount of information. However, for a computer to analyze this information the interferogram data must be transferred to the computer. Twenty or thirty years ago the approach was to take a static interferogram and use a graphics tablet or densitometer to find the fringe centers and transfer this fringe center information to a computer first using IBM punch cards and later directly interfacing the graphics tablet or densitometer to the computer. Since normally the analysis required data on a regular grid, interpolation or polynomial fitting was used to go from fringe centers to the grid. Typically only 100-200 data points would be used. Additional information was required to get the polarity of the wavefront. While today the idea of using only fringe center data to determine wavefronts seems very archaic, at the time it was a large advance forward enabling the fabrication of better optical components and optical systems.

A much better approach for getting interferogram data into a computer is to take a series of interferograms while the phase difference between the two interfering beams changes. The wavefront phase distribution is encoded in the irradiance variation, and as will be shown below, the wavefront phase difference between the two interfering beams can be obtained by analyzing the point by point irradiance of three or more interferograms as the phase difference is varied. This method

for obtaining phase information from interferograms is now known as phase-shifting interferometry (PSI).

The concept of PSI has been used for a long time in electrical engineering for determining the phase difference between two electrical signals and is called synchronous detection. In the 1960s many researchers began using PSI approaches and the earliest reference on the subject is believed to be in 1966 (Carré, 1966). While many others worked on the topic in the 1960s and 1970s little was published because most of the work was concerned with either defense or company proprietary projects (Crane 1969; Bruning et al. 1974; Wyant 1975; Hardy et al. 1977). The topic did not become really popular until the 1980s when good quality CCDs and small powerful computers became available. At the present time most serious interferometric metrology work involves phase-shifting techniques.

Two excellent review book chapters have been written on PSI (Creath 1988; Greivenkamp and Bruning 1992). These notes are not intended to replace these review chapters, but rather they are intended to supply the basic PSI concepts in an interactive form where the reader can not only learn the basic concepts but also try new ideas. Below we will discuss the basic concepts of phase-shifting interferometry followed by discussion and derivation of the basic algorithms, discussion of error sources, and a description of the phase-shifters required.

## 3 Basic Concepts of PSI

---

### 3.1 Two Beam Interference and 4-Step PSI Algorithm

The basic equation for two-beam interference is

$$\text{irradiance}[x, y] = i_a + i_b \text{Cos}[\theta[x, y]]$$

or

$$\text{irradiance}[x, y] = i_{avg} (1 + \gamma \text{Cos}[\theta[x, y]])$$

Let  $\theta[x,y]$  be equal to a constant value,  $\delta$ , which we will call a piston term, and a variable  $\phi[x,y]$  which depends upon position  $x, y$ . The irradiance can be written as

$$\text{irradiance}[x, y, \delta] = i_{avg} (1 + \gamma \text{Cos}[\phi[x, y] + \delta]). \quad (1)$$

While the above is the most common way of writing the irradiance distribution for two-beam interference, it is often convenient to rewrite  $\text{Cos}[\phi + \delta]$  as a product of  $\text{Cos}[\phi] \text{Cos}[\delta]$  and  $\text{Sin}[\phi] \text{Sin}[\delta]$ . That is,

$$\mathbf{TrigExpand}[i_{avg} (1 + \gamma \text{Cos}[\phi[x, y] + \delta])]$$

$$i_{avg} + i_{avg} \gamma \text{Cos}[\delta] \text{Cos}[\phi[x, y]] - i_{avg} \gamma \text{Sin}[\delta] \text{Sin}[\phi[x, y]]$$

Letting

$$a_0 = i_{avg}$$

$$a_1 = i_{avg} \gamma \text{Cos}[\delta] \text{Cos}[\phi[x, y]]$$

$$a_2 = - i_{avg} \gamma \text{Sin}[\delta] \text{Sin}[\phi[x, y]]$$

we can write

---


$$\text{irradiance} = a_0 + a_1 \text{Cos}[\delta] + a_2 \text{Sin}[\delta] \quad (2)$$

It is important to note that

$$\text{Tan}[\phi] = \frac{-a_2}{a_1} \quad (3)$$

and

$$\gamma = \frac{\sqrt{a_1^2 + a_2^2}}{a_0} \quad (4)$$

Equations 2 and 3 are the two most useful equations in PSI.

It is also important that not only do we determine the tangent of the phase, but also the individual sine and cosine are determined. This means that we know which quadrant the phase is in, so when the arctangent is performed the phase is determined from  $-\pi$  to  $\pi$ . As will be shown below, if we set a limit on the slope of the phase being measured that the phase difference between adjacent detector points is less than  $\pi$ , then we will be able to extend the range of the phase measurement by correcting for the  $2\pi$  ambiguities in the arctangent calculation.

The easiest way of understanding the concept of phase-shifting interferometry is to look at what is commonly called the four-step algorithm. As stated above, the irradiance can be written either as

$$\text{irradiance}[n\_] := a_0 + a_1 \text{Cos}[\delta[n]] + a_2 \text{Sin}[\delta[n]]$$

or as

$$i[n\_] := i_{\text{avg}} (1 + \gamma \text{Cos}[\phi + \delta[n]])$$

Normally we will use the first expression for the irradiance, but in this case we will use the second expression.

Let  $\delta$  have four values.

$$\delta[1] = 0; \delta[2] = \frac{\pi}{2}; \delta[3] = \pi; \delta[4] = \frac{3\pi}{2};$$

$$i[1] /. \delta[1] \rightarrow 0$$

$$i_{\text{avg}} (1 + \gamma \text{Cos}[\phi])$$

$$i[2] /. \delta[2] \rightarrow \frac{\pi}{2}$$

$$i_{\text{avg}} (1 - \gamma \text{Sin}[\phi])$$

$$i[3] /. \delta[3] \rightarrow \pi$$

$$i_{\text{avg}} (1 - \gamma \text{Cos}[\phi])$$

$$i[4] /. \delta[4] \rightarrow \frac{3\pi}{2}$$

$$i_{\text{avg}} (1 + \gamma \text{Sin}[\phi])$$

It is clear that

$$\text{Simplify}\left[\frac{i[4] - i[2]}{i[1] - i[3]}\right] /. \{\delta[1] \rightarrow 0, \delta[2] \rightarrow \frac{\pi}{2}, \delta[3] \rightarrow \pi, \delta[4] \rightarrow \frac{3\pi}{2}\}$$

$$\text{Tan}[\phi]$$

That is,

$$\text{Tan}[\phi] = \frac{i[4] - i[2]}{i[1] - i[3]}. \quad (5)$$

This is a very powerful algorithm. Remembering that this calculation is performed for each detector point we see that by taking the difference any fixed pattern noise is eliminated. Due to the division detector sensitivity variations and irradiance variations across the beam have no effect on the result except changing the signal to noise.

### 3.2 Phase-shifting (integrated bucket) vs phase-stepping

In the four-step method shown above the phase difference is changed in discrete steps. For practical reasons it is generally better to vary the phase at a constant rate. If the phase is changed in discrete steps a delay is required after each phase step to reduce effects of ringing in the phase shifter and the phase shifting electronics. Because of environmental factors the data needs to be taken as fast as possible and delays after each phase step are unacceptable in most situations. The phase-shift or integrated bucket technique (Wyant, 1975) allows the phase difference to vary linearly in time, and as shown below the only penalty for allowing the phase difference to vary during the detector integration time is a small reduction in the fringe visibility. This integration time is normally equal to the frame time of the detector, but it can be equal to a shorter time if the time required to collect an adequate signal is shorter than the frame time.

Let  $\Delta$  be the integration time, then the signal can be written as

$$\text{signal} = \frac{1}{\Delta} \int_{\delta[n]-\Delta/2}^{\delta[n]+\Delta/2} (i\text{avg} (1 + \gamma \text{Cos}[\phi[\mathbf{x}, \mathbf{y}] + \delta])) d\delta;$$

$$\text{signal} = \text{FullSimplify}[\text{signal}]$$

$$i\text{avg} + \frac{2 i\text{avg} \gamma \text{Cos}[\delta[n] + \phi[\mathbf{x}, \mathbf{y}]] \text{Sin}[\frac{\Delta}{2}]}{\Delta}$$

$$\text{signal} = \text{Factor}\left[\text{signal} /. \frac{2 \text{Sin}[\frac{\Delta}{2}]}{\Delta} \rightarrow \text{sinc}\left[\frac{\Delta}{2}\right]\right]$$

$$i\text{avg} (1 + \gamma \text{Cos}[\delta[n] + \phi[\mathbf{x}, \mathbf{y}]] \text{sinc}\left[\frac{\Delta}{2}\right]) \quad (6)$$

Thus, as shown by Equation 6 the effect of integrating the irradiance as the phase is continuously varied is to reduce the contrast of the signal by an amount equal to  $\text{sinc}\left[\frac{\Delta}{2}\right]$ . Normally, this reduction in contrast is negligible. For example, if the irradiance is integrated as the phase changes by  $\frac{\pi}{2}$  the contrast is reduced by

$$\frac{\text{Sin}\left[\frac{\Delta}{2}\right]}{\frac{\Delta}{2}} /. \Delta \rightarrow \frac{\pi}{2} // \mathbf{N}$$

$$0.900316$$

Generally the 10 % reduction in fringe contrast is acceptable and the integrated bucket approach is used instead of phase stepping since the data can be taken faster.

It should be noted that since the only effect of integrating the irradiance as the phase changes is a fringe contrast reduction, the same phase algorithms are valid for both the phase-stepping and the integrated bucket approach.

### 3.3 Phase unwrapping

Since the phase is calculated from an arctangent there are discontinuities in the phase calculation. Normally the arctangent is defined only over a range of  $-\pi/2$  to  $\pi/2$ . However, in phase-shifting interferometry we know the signs of the individual sines and cosines. This means that we know which quadrant the phase is in, so when the arctangent is performed the phase is determined over a range of  $-\pi$  to  $\pi$ .

The range of phase that can be measured can be further extended if we set a limit on the slope of the measured phase such that the phase difference between adjacent detector points is less than  $\pi$ . The phase difference between adjacent detector points can then be calculated and when the calculated phase difference is greater than  $\pi$  we know that the phase difference is calculated too large because of  $2\pi$  ambiguities in the arctangent. The  $2\pi$  ambiguity is corrected by adding or subtracting  $2\pi$  to the phase of one of the data points so the phase difference is less than  $\pi$ . This process needs to be repeated for all data points until the phase difference between all adjacent data points is less than  $\pi$ .

The phase unwrapping module in Section 8.4 can be used to correct for  $2\pi$  phase ambiguities for one-dimensional phase data. In practice, two-dimensional phase unwrapping algorithms work along the same principle, but they can be more difficult to implement because of obscurations in the data and noise. Care must be taken that all data points have the  $2\pi$  ambiguity correction applied. The best phase unwrapping algorithms look at the contrast of the signal at each data point and unwraps the phase at the highest contrast, lowest noise, points first. The effects of errors in the unwrapping leads to streaks in the data where the unwrapping is incorrect.

## 4 Basic Algorithms

---

### 4.1 Three-Step Algorithms

The goal is to find  $\phi[x,y]$ . If we measure the irradiance and we know  $\delta$ , we are left with three unknowns,  $a_0$ ,  $a_1$ , and  $a_2$ . Since there are three unknowns, three measurements of the irradiance for three different values of  $\delta$  are required. Let

$$\text{irradiance}[n\_ ] := a_0 + a_1 \text{Cos}[\delta[n]] + a_2 \text{Sin}[\delta[n]]$$

Let the three irradiance measurements for the three different values of  $\delta$  be  $\text{imeasured}[1]$ ,  $\text{imeasured}[2]$ , and  $\text{imeasured}[3]$ .

We will now look at a few three-step algorithms.

#### 4.1.1 Three-Step Algorithm, Example 1

For the first example let the three values of  $\delta$  be  $\frac{\pi}{4}$ ,  $\frac{3\pi}{4}$ , and  $\frac{5\pi}{4}$ . Solving for  $a_1$  and  $a_2$  yields

```

ans =
Simplify[Solve[{irradiance[1] == imeasured[1], irradiance[2] == imeasured[2],
irradiance[3] == imeasured[3]}, {a1, a2}, {a0, a2}] /.
{δ[1] →  $\frac{\pi}{4}$ , δ[2] →  $\frac{3\pi}{4}$ , δ[3] →  $\frac{5\pi}{4}$ }]
{{a1 →  $\frac{\text{imeasured}[1] - \text{imeasured}[2]}{\sqrt{2}}$ , a2 →  $\frac{\text{imeasured}[2] - \text{imeasured}[3]}{\sqrt{2}}$ }}

tanPhase =  $\frac{-a2 /. \text{ans}[[1]]}{a1 /. \text{ans}[[1]]}$ 
 $-\frac{\text{imeasured}[2] - \text{imeasured}[3]}{\text{imeasured}[1] - \text{imeasured}[2]}$ 

```

Thus,

$$\text{Tan}[\phi] = -\frac{\text{imeasured}[2] - \text{imeasured}[3]}{\text{imeasured}[1] - \text{imeasured}[2]} \quad (7)$$

#### 4.1.2 Three-Step Algorithm, Example 2

For the second example let the three values of  $\delta$  be  $-\frac{\pi}{2}$ , 0, and  $\frac{\pi}{2}$ . Solving for a1 and a2 yields

```

ans =
Simplify[Solve[{irradiance[1] == imeasured[1], irradiance[2] == imeasured[2],
irradiance[3] == imeasured[3]}, {a1, a2},
{a0, a1, a2}] /. {δ[1] →  $-\frac{\pi}{2}$ , δ[2] → 0, δ[3] →  $\frac{\pi}{2}$ }]
{{a1 →  $\frac{1}{2} (-\text{imeasured}[1] + 2 \text{imeasured}[2] - \text{imeasured}[3])$ ,
a2 →  $\frac{1}{2} (-\text{imeasured}[1] + \text{imeasured}[3])$ }}

tanPhase =  $\frac{-a2 /. \text{ans}[[1]]}{a1 /. \text{ans}[[1]]}$ 
 $\frac{\text{imeasured}[1] - \text{imeasured}[3]}{-\text{imeasured}[1] + 2 \text{imeasured}[2] - \text{imeasured}[3]}$ 

```

Thus,

$$\text{Tan}[\phi] = \frac{\text{imeasured}[1] - \text{imeasured}[3]}{-\text{imeasured}[1] + 2 \text{imeasured}[2] - \text{imeasured}[3]} \quad (8)$$

#### 4.1.3 Three-Step Algorithm, Example 3

For the third example let the three values of  $\delta$  be  $-\alpha$ , 0, and  $\alpha$ . Solving for a1 and a2 yields

```

ans = FullSimplify[
  Solve[{irradiance[1] == imeasured[1], irradiance[2] == imeasured[2],
    irradiance[3] == imeasured[3]}, {a1, a2},
    {a0, a2}] /. {δ[1] → -α, δ[2] → 0, δ[3] → α}

  {{a1 →  $\frac{\text{imeasured}[1] - 2 \text{imeasured}[2] + \text{imeasured}[3]}{-2 + 2 \text{Cos}[\alpha]}$ ,
    a2 →  $\frac{1}{2} \text{Csc}[\alpha] (-\text{imeasured}[1] + \text{imeasured}[3])$ }}

tanPhase = Simplify[ $\frac{-a2 /. \text{ans}[[1]]}{a1 /. \text{ans}[[1]]}$ ]

 $\frac{(-1 + \text{Cos}[\alpha]) \text{Csc}[\alpha] (\text{imeasured}[1] - \text{imeasured}[3])}{\text{imeasured}[1] - 2 \text{imeasured}[2] + \text{imeasured}[3]}$ 

tanPhase =  $\frac{\text{TrigFactor}[-1 + \text{Cos}[\alpha] \text{Csc}[\alpha] ] (\text{imeasured}[1] - \text{imeasured}[3])}{\text{imeasured}[1] - 2 \text{imeasured}[2] + \text{imeasured}[3]}$ 

 $-\frac{(\text{imeasured}[1] - \text{imeasured}[3]) \text{Tan}[\frac{\alpha}{2}]}{\text{imeasured}[1] - 2 \text{imeasured}[2] + \text{imeasured}[3]}$ 

```

Thus,

$$\text{Tan}[\phi] = -\frac{(\text{imeasured}[1] - \text{imeasured}[3]) \text{Tan}[\frac{\alpha}{2}]}{\text{imeasured}[1] - 2 \text{imeasured}[2] + \text{imeasured}[3]} \quad (9)$$

If  $\alpha = \frac{\pi}{2}$  we get the same result as given in example 2.

It should be noted that for all three examples not only do we get the tangent of the phase, but we also determine the sine and cosine. As discussed in Section 3.3 this is important for correcting phase ambiguities.

#### 4.1.4 2+1 Algorithm, (Angel and Wizinowich)

The 2 + 1 algorithm first described by Angel and Wizinowich (Angel and Wizinowich 1988; Wizinowich 1989, 1990) is a very clever approach for attacking the problem of measurement errors introduced by vibration. In the 2 + 1 approach two interferograms having a 90 degree phase shift are rapidly collected and later a third interferogram is collected that is the average of two interferograms with a 180 degree phase shift. The phase shifts are thus 0,  $-\pi/2$ , and 0 and  $\pi$ . Since

$$\text{irradiance}[n\_ ] := a0 + a1 \text{Cos}[\delta[n]] + a2 \text{Sin}[\delta[n]]$$

the three irradiance patterns can be written as

$$\text{irradiance}[1] := a0 + a1 \text{Cos}[\delta[1]] + a2 \text{Sin}[\delta[1]] \quad /. \delta[1] \rightarrow 0$$

$$\text{irradiance}[2] := a0 + a1 \text{Cos}[\delta[2]] + a2 \text{Sin}[\delta[2]] \quad /. \delta[2] \rightarrow \frac{-\pi}{2}$$

```

irradiance[3] :=
  1
  --- (a0 + a1 Cos[δ[3]] + a2 Sin[δ[3]] + a0 + a1 Cos[δ[4]] + a2 Sin[δ[4]]) /.
  2
  {δ[3] → 0, δ[4] → π}

irradiance[1]

a0 + a1

irradiance[2]

a0 - a2

irradiance[3]

a0

```

The answer is so simple we could write it down by inspection, but we will let *Mathematica* solve for *tanPhase*.

```

ans = Solve[{irradiance[1] == imeasured[1], irradiance[2] == imeasured[2],
  irradiance[3] == imeasured[3]}, {a1, a2}, {a0, a2}];

tanPhase = Simplify[ $\frac{-a2 /. ans[[1]]}{a1 /. ans[[1]]}$ ]


$$\frac{\text{imeasured}[2] - \text{imeasured}[3]}{\text{imeasured}[1] - \text{imeasured}[3]}$$


```

The result is not surprising.

The nice thing about the Angel-Wizinowich approach is their clever implementation for using an interline transfer CCD for rapidly obtaining the two interferograms having the  $90^\circ$  phase shift. In an interline transfer CCD each photosite is accompanied by an adjacent storage pixel. The storage pixels are read out to produce the video signal while the active photosites are integrating the light for the next video field. After exposure, the charge collected in the active pixels is transferred in a microsecond to the now empty storage sites, and the next video field is collected. It is possible to synchronize a shutter to the sensor to record two exposures of about a millisecond in duration separated by a microsecond. One exposure is made just before the transfer and the second is recorded just after the transfer. The two recorded interferograms are read out at standard video rates. A  $90^\circ$  phase shift is made before the two exposures. In the Angel-Wizinowich approach two orthogonally polarized light beams were produced having two sets of interference fringes  $90^\circ$  out of phase. A Pockel cell was used to select which set of fringes was present on the detector. Between the two exposures the Pockel cell was switched to change the fringes present on the detector. The third exposure is made with two sets of fringes  $180^\circ$  degrees out of step present. In this case the Pockel cell is switched to allow both orthogonal polarizations present on the detector at the same time.

While the Angel-Wizinowich approach is very clever, it has found limited use because the small number of data frames in the  $2 + 1$  algorithm makes it susceptible to errors resulting from phase-shifter nonlinearity and calibration.

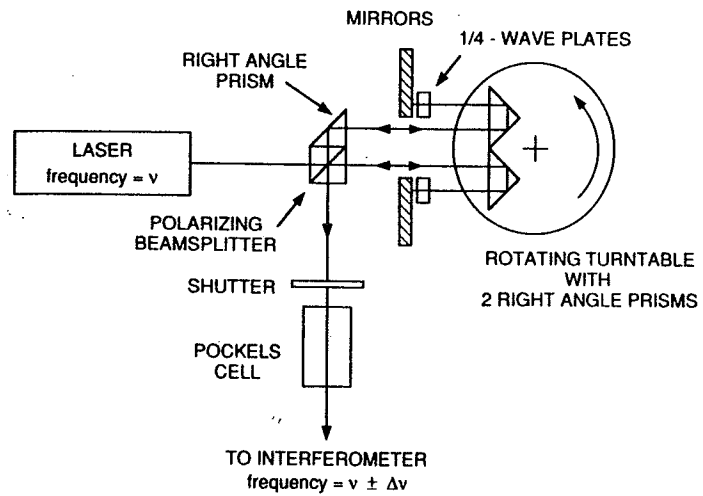


**Figure 14.10.** The system used to generate the phase shifts required for the  $2 + 1$  algorithm. (From Wizinowich 1990).

## 4.2 Carré Algorithm

Carré is generally given credit for being the first to publish on PSI (Carré 1966). While the Carré algorithm is seldom used because small amounts of phase shifting nonlinearity can introduce large error in the measurements, it is interesting for historical reasons.

In the Carré algorithm the phase shift between consecutive measurements is treated as an unknown and solved for in the analysis. A linear phase shift of  $2\alpha$  is assumed between each step so the phase steps are assumed to be  $-3\alpha$ ,  $-\alpha$ ,  $\alpha$ , and  $3\alpha$ . The four measured irradiance frames are now represented by

$$\text{irradiance}[1] := a_0 + a_1 \cos[\delta[1]] + a_2 \sin[\delta[1]] \quad / . \quad \delta[1] \rightarrow -3\alpha$$

$$\text{irradiance}[2] := a_0 + a_1 \cos[\delta[2]] + a_2 \sin[\delta[2]] \quad / . \quad \delta[2] \rightarrow -\alpha$$

$$\text{irradiance}[3] := a_0 + a_1 \cos[\delta[3]] + a_2 \sin[\delta[3]] \quad / . \quad \delta[3] \rightarrow \alpha$$

$$\text{irradiance}[4] := a_0 + a_1 \cos[\delta[4]] + a_2 \sin[\delta[4]] \quad / . \quad \delta[4] \rightarrow 3\alpha$$

**irradiance[1]**

$$a_0 + a_1 \cos[3\alpha] - a_2 \sin[3\alpha]$$

**irradiance[2]**

$$a_0 + a_1 \cos[\alpha] - a_2 \sin[\alpha]$$

**irradiance[3]**

$$a_0 + a_1 \cos[\alpha] + a_2 \sin[\alpha]$$

**irradiance[4]**

$$a_0 + a_1 \cos[3\alpha] + a_2 \sin[3\alpha]$$

Since for this example we do not know the phase shift,  $2\alpha$ , we have four unknowns. Fortunately we also have four equations. The solution is a little messy. We know that

$$\tan[\phi] = \frac{-a_2}{a_1}$$

Looking at the above equations we can intelligently guess that we want to find

$$\text{Simplify}\left[\frac{(\text{irradiance}[1] - \text{irradiance}[4]) + (\text{irradiance}[2] - \text{irradiance}[3])}{-(\text{irradiance}[1] + \text{irradiance}[4]) + (\text{irradiance}[2] + \text{irradiance}[3])}\right]$$

$$-\frac{a_2 \cot[\alpha]}{a_1}$$

Thus,

$$\tan\text{Phase} = \frac{\tan[\alpha] \left( (\text{irradiance}[1] - \text{irradiance}[4]) + (\text{irradiance}[2] - \text{irradiance}[3]) \right)}{-(\text{irradiance}[1] + \text{irradiance}[4]) + (\text{irradiance}[2] + \text{irradiance}[3])}$$

Now we must solve for  $\tan[\alpha]$ . Rather than solving directly for  $\tan[\alpha]$  we will prove that the answer given in Carré's paper is correct.

$$\tan\text{Alpha} = \text{Sqrt}\left[ \text{Simplify}\left[ \frac{3 (\text{irradiance}[2] - \text{irradiance}[3]) - (\text{irradiance}[1] - \text{irradiance}[4])}{(\text{irradiance}[1] - \text{irradiance}[4]) + (\text{irradiance}[2] - \text{irradiance}[3])} \right] \right]$$

$$\sqrt{\tan[\alpha]^2}$$

Letting  $\text{irradiance}[n] = i_n$  we have

$$\tan\text{Phase} = \frac{\sqrt{(3 (i_2 - i_3) - (i_1 - i_4)) ((i_1 - i_4) + (i_2 - i_3))}}{(i_2 + i_3) - (i_1 + i_4)}$$

While the Carré algorithm is convenient because the value of the phase shift is not very important as long as the phase shift between consecutive frames is a constant, the algorithm is seldom used because nonlinearities in the phase shift introduce large errors in the measurements.

## 5 Least Squares Approach for Finding Algorithms

While only three irradiance measurements are required, generally more than three measurements are made to reduce the errors due to phase steps being incorrect, detector non-linearities, electronic noise, air turbulence, vibration, etc. One way to determine the phase if more than three irradiance measurements are made is to use a least squares fit of the data as described by several authors including (Bruning 1974; Morgan 1982; Greivenkamp 1984; Phillion 1997). The algorithms obtained using the least-squares approach are similar to the best algorithms obtained by several other authors (Hariharan, 1987; Freischlad and Koliopoulos 1990; Schmit and Creath 1995; de Groot 1995).

The least squares approach is very powerful. Using least squares three or more phase step values can be used to measure the wavefront. These values do not need to be evenly spaced and can be spread over a range greater than  $2\pi$ . However, the choice of phase shift positions will influence the phase measurement accuracy. Also, as will be shown below, weighting factors can be applied to the different squared differences before the differentiation is performed. These weighting factors can be tuned to minimize errors due to incorrect phase shifts and detector nonlinearities.

The normal procedure for performing the least squares fit is to first find the square of the difference between the measured irradiance and the irradiance predicted using the normal sinusoidal irradiance relationship given above. This error is minimized by differentiating with respect to each of the three unknowns and equating these results to zero. The simultaneous solution of these three equations produces the least square result. We will obtain this simultaneous solution using the *Mathematica* function `Solve`. The tangent of the phase is then calculated as  $-a2/a1$ .

The following shows a few examples:

### 5.1 Four steps

An algorithm for four-steps was derived above. We will now use the least squares approach to derive a four-step algorithm. It will turn out to be the same algorithm derived above.

```

numberSteps = 4;
esquared = Sum[(imeasured[i] - irradiance[i])2, {i, 1, numberSteps}];
d0 = D[esquared, a0];
d1 = D[esquared, a1];
d2 = D[esquared, a2];

ans = Simplify[Solve[{d0 == 0, d1 == 0, d2 == 0}, {a0, a1, a2}, {a0, a1, a2}] /.
Table[ $\delta[i] \rightarrow (i - 1) \frac{\pi}{2}$ , {i, 1, numberSteps}]]]

{ {a0  $\rightarrow \frac{1}{4}$  (imeasured[1] + imeasured[2] + imeasured[3] + imeasured[4]),
  a1  $\rightarrow \frac{1}{2}$  (imeasured[1] - imeasured[3]), a2  $\rightarrow \frac{1}{2}$  (imeasured[2] - imeasured[4]) } }

```

$$\text{tanPhase} = \text{FullSimplify}\left[\frac{-a2 /. \text{ans}[[1]]}{a1 /. \text{ans}[[1]]}\right]$$

$$\frac{-\text{imeasured}[2] + \text{imeasured}[4]}{\text{imeasured}[1] - \text{imeasured}[3]}$$

This is the same result as derived above.

We will now solve for the fringe contrast, gamma.

$$\text{gamma} = \text{FullSimplify}\left[\frac{\sqrt{(a1 /. \text{ans}[[1]])^2 + (a2 /. \text{ans}[[1]])^2}}{a0 /. \text{ans}[[1]]}\right]$$

$$\frac{2 \sqrt{(\text{imeasured}[1] - \text{imeasured}[3])^2 + (\text{imeasured}[2] - \text{imeasured}[4])^2}}{\text{imeasured}[1] + \text{imeasured}[2] + \text{imeasured}[3] + \text{imeasured}[4]}$$

## 5.2 Synchronous Detection

In communication theory synchronous detection is used to detect a noisy signal by correlating it with sinusoidal and cosinusoidal signals of the same frequency and averaged over many periods of oscillation. The method of synchronous detection was applied to PSI by Bruning et al. (Bruning 1974). It is very interesting that if the irradiance measurements are equally spaced over  $2\pi$ , synchronous detection and least squares give the same result.

The basic equation for synchronous detection is

$$\text{tanPhase}[n_] := -\frac{\sum_{i=1}^n \text{imeasured}[i] \text{Sin}\left[i \frac{2\pi}{n}\right]}{\sum_{i=1}^n \text{imeasured}[i] \text{Cos}\left[i \frac{2\pi}{n}\right]}$$

As an example let  $n=3$ .

**Simplify[tanPhase[3]]**

$$\frac{\sqrt{3} (\text{imeasured}[1] - \text{imeasured}[2])}{\text{imeasured}[1] + \text{imeasured}[2] - 2 \text{imeasured}[3]}$$

**Clear[tanPhase]**

Now we will go through the derivation using the least squares approach.

```

numberSteps = 3;
esquared = Sum[(imeasured[i] - irradiance[i])^2, {i, 1, numberSteps}];
d0 = D[esquared, a0];
d1 = D[esquared, a1];
d2 = D[esquared, a2];

```

```

ans = Simplify[Solve[{d0 == 0, d1 == 0, d2 == 0}, {a0, a1, a2}, {a0, a1, a2}] /.
  Table[δ[i] → (i)  $\frac{2\pi}{\text{numberSteps}}$ , {i, 1, numberSteps}]];

tanPhase = Simplify[ $\frac{-a2 /. \text{ans}[[1]]}{a1 /. \text{ans}[[1]]}$ ]


$$\frac{\sqrt{3} (\text{imeasured}[1] - \text{imeasured}[2])}{\text{imeasured}[1] + \text{imeasured}[2] - 2 \text{imeasured}[3]}$$


```

The results are the same for synchronous detection and least squares. If we used more steps evenly spaced over  $2\pi$  we would find that synchronous detection and least squares give the same result.

### 5.3 Five steps

Five step algorithms offer advantages in reduced sensitivity to phase shifter calibration.

```

numberSteps = 5;
esquared = Sum[(imeasured[i] - irradiance[i])2, {i, 1, numberSteps}];
d0 = D[esquared, a0];
d1 = D[esquared, a1];
d2 = D[esquared, a2];

ans = Simplify[Solve[{d0 == 0, d1 == 0, d2 == 0}, {a0, a1, a2}, {a0, a1, a2}] /.
  Table[δ[i] → (i - 3)  $\frac{\pi}{2}$ , {i, 1, numberSteps}]]

{{a0 →  $\frac{1}{14} (2 \text{imeasured}[1] + 3 \text{imeasured}[2] + 4 \text{imeasured}[3] + 3 \text{imeasured}[4] + 2 \text{imeasured}[5])$ ,
  a1 →  $\frac{1}{14} (-4 \text{imeasured}[1] + \text{imeasured}[2] + 6 \text{imeasured}[3] + \text{imeasured}[4] - 4 \text{imeasured}[5])$ ,
  a2 →  $\frac{1}{2} (-\text{imeasured}[2] + \text{imeasured}[4])$ }}

tanPhase = FullSimplify[ $\frac{-a2 /. \text{ans}[[1]]}{a1 /. \text{ans}[[1]]}$ ]


$$\frac{7 (\text{imeasured}[2] - \text{imeasured}[4])}{-4 \text{imeasured}[1] + \text{imeasured}[2] + 6 \text{imeasured}[3] + \text{imeasured}[4] - 4 \text{imeasured}[5]}$$


gamma = FullSimplify[ $\frac{\sqrt{(a1 /. \text{ans}[[1]])^2 + (a2 /. \text{ans}[[1]])^2}}{a0 /. \text{ans}[[1]]}$ ]

```

$$\frac{\left(\sqrt{(49 (\text{imeasured}[2] - \text{imeasured}[4])^2 + (-4 \text{imeasured}[1] + \text{imeasured}[2] + 6 \text{imeasured}[3] + \text{imeasured}[4] - 4 \text{imeasured}[5])^2)}\right)}{(2 \text{imeasured}[1] + 3 \text{imeasured}[2] + 4 \text{imeasured}[3] + 3 \text{imeasured}[4] + 2 \text{imeasured}[5])}$$

## 5.4 Five steps (Schwider-Hariharan Algorithm)

In the five-step approach given above `imeasured[5]` and `imeasured[1]` are nominally identical and differ only because of measurement errors. For this reason, in performing the least-squares fit it makes sense to give one-half as much weight to `imeasured[5]` and `imeasured[1]` as is given to the other measurements. The resulting algorithm we will derive was first described by Schwider (Schwider 1983) and later by Hariharan (Hariharan, Oreb, and Eiju 1987) and as shown in Section 6.1.4 it is less sensitive to errors in the 90 degree phase shift than the algorithms given above.

```
a[1] = 1; a[2] = 2; a[3] = 2; a[4] = 2; a[5] = 1;
```

```
numberSteps = 5;
```

```
esquared = Sum[a[i] (imeasured[i] - irradiance[i])^2, {i, 1, numberSteps}];
```

```
d0 = D[esquared, a0];
```

```
d1 = D[esquared, a1];
```

```
d2 = D[esquared, a2];
```

```
ans = Simplify[Solve[{d0 == 0, d1 == 0, d2 == 0}, {a0, a1, a2}, {a0, a1, a2}] /.
```

```
Table[δ[i] → (i - 3)  $\frac{\pi}{2}$ , {i, 1, numberSteps}]]];
```

```
tanPhase = FullSimplify[ $\frac{-a2 /. ans[[1]]}{a1 /. ans[[1]]}$ ]
```

$$-\frac{2 (\text{imeasured}[2] - \text{imeasured}[4])}{\text{imeasured}[1] - 2 \text{imeasured}[3] + \text{imeasured}[5]}$$

```
gamma = FullSimplify[ $\frac{\sqrt{(a1 /. ans[[1]])^2 + (a2 /. ans[[1]])^2}}{a0 /. ans[[1]]}$ ]
```

$$\frac{\left(2 \sqrt{(4 (\text{imeasured}[2] - \text{imeasured}[4])^2 + (\text{imeasured}[1] - 2 \text{imeasured}[3] + \text{imeasured}[5])^2)}\right)}{(\text{imeasured}[1] + 2 (\text{imeasured}[2] + \text{imeasured}[3] + \text{imeasured}[4]) + \text{imeasured}[5])}$$

## 5.5 Weighted Coefficients - Improved Algorithms

During the past 15 years there have been numerous publications concerning better phase-shifting algorithms. However, most, if not all of the best algorithms follow a procedure suggested by Schwider (Schwider 1983). First, Schwider pointed out that many of the errors, especially errors due to phase shifter miscalibration, occur at twice the frequency of the interference fringes. Therefore, he said to perform the measurement twice with a  $90^\circ$  offset in the phase shift and then average the two results having errors  $180^\circ$  out of phase to nearly cancel the double frequency error. Furthermore, we did not have to actually perform the measurement twice, but as long as the phase step was  $90^\circ$  all we had to do was to add one more frame of data and use frames 1 thru N-1 for the first calculation and frames 2 thru N for the second calculation and average the two results. The result had greatly reduced error due to phase shifter calibration.

While the above approach for averaging two  $90^\circ$  offset phase measurements was well known by people working in phase shifting interferometry long before Schwider's publication, Schwider made another more significant observation in his paper that was not well known. Schwider showed that rather than averaging the calculated phase after the arctangent was performed, the numerators and the denominators of the arctangent function could be averaged. That is, if two data sets are taken with a  $90^\circ$  phase step between the two data sets the phase calculation can be of the form

$$\text{Tan}[\phi] = \frac{n_1 + n_2}{d_1 + d_2}$$

where  $n_i$  and  $d_i$  are the numerator and denominator for phase calculation algorithm for each data set. If the phase step is  $\pi/2$ , only one additional data frame is required.  $n_1$  and  $d_1$  are calculated from frames 1 thru N-1 and  $n_2$  and  $d_2$  are calculated from frames 2 thru N.

The Schwider-Hariharan algorithm presented above is an example of this approach. The 4-step algorithm calculated above was

$$\text{tanphase} = \frac{-\text{imeasured}[2] + \text{imeasured}[4]}{\text{imeasured}[1] - \text{imeasured}[3]}$$

If we took another frame and used frames 2 thru 5 the algorithm would be

$$\text{tanphase} = \frac{-\text{imeasured}[2] + \text{imeasured}[4]}{\text{imeasured}[5] - \text{imeasured}[3]}$$

If we use the Schwider approach and added the numerators and denominators we would have

$$\text{tanphase} = \frac{2(-\text{imeasured}[2] + \text{imeasured}[4])}{\text{imeasured}[1] - 2\text{imeasured}[3] + \text{imeasured}[5]}$$

which is the Schwider-Hariharan algorithm which exhibits much less error due to phase shifter calibration than the 4-step algorithm, and it is better, and faster, than calculating the phase using two  $\pi/2$  offset 4-frame algorithms and averaging the results.

We could now add another data frame and repeat the procedure to obtain an even better 6-frame algorithm. Then of course we could add yet another frame and get an even better 7-frame algorithm. However, rather than going through all the algebra a better way is to do a weighted coefficient least squares fit and let the computer do the work. We will start with the 4 frame algorithm where all the weighting factors are one. Let numberSteps be equal to the number of frames or phase steps, then the  $i$ th coefficient can be written as  $a[i, \text{numberSteps}]$ . Using the Schweider approach

```

a[1, numberSteps] =
  a[numberSteps, numberSteps] = 1 and for all other values of i
a[i, numberSteps] = a[i - 1, numberSteps - 1] + a[i, numberSteps - 1]

```

These values of a are then used as the weighting coefficients as demonstrated below for the situation where numberSteps = 6.

```

numberSteps = 6;

Do[a[i, 4] = 1, {i, 1, 4}];
  Do[Do[If[i == 1 || i == numberSteps, a[i, numberSteps] = 1,
    a[i, numberSteps] = a[i - 1, numberSteps - 1] + a[i, numberSteps - 1]],
    {i, 1, numberSteps}], {numberSteps, 5, 13}];

esquared =
  Sum[a[i, numberSteps] (imeasured[i] - irradiance[i])2, {i, 1, numberSteps}];
d0 = D[esquared, a0];
d1 = D[esquared, a1];
d2 = D[esquared, a2];

ans = Simplify[Solve[{d0 == 0, d1 == 0, d2 == 0}, {a0, a1, a2}, {a0, a1, a2}] /.
  Table[δ[i] → (i - 3)  $\frac{\pi}{2}$ , {i, 1, numberSteps}]];

tanPhase = FullSimplify[ $\frac{-a2 /. ans[[1]]}{a1 /. ans[[1]]}$ ]

$$-\frac{3 \text{imeasured}[2] - 4 \text{imeasured}[4] + \text{imeasured}[6]}{\text{imeasured}[1] - 4 \text{imeasured}[3] + 3 \text{imeasured}[5]}$$


```

Just as easily we can calculate the algorithm for 7 steps.

```

numberSteps = 7;

Do[a[i, 4] = 1, {i, 1, 4}];
  Do[Do[If[i == 1 || i == numberSteps, a[i, numberSteps] = 1,
    a[i, numberSteps] = a[i - 1, numberSteps - 1] + a[i, numberSteps - 1]],
    {i, 1, numberSteps}], {numberSteps, 5, 13}];

esquared =
  Sum[a[i, numberSteps] (imeasured[i] - irradiance[i])2, {i, 1, numberSteps}];
d0 = D[esquared, a0];
d1 = D[esquared, a1];
d2 = D[esquared, a2];

```

---

```

ans = Simplify[Solve[{d0 == 0, d1 == 0, d2 == 0}, {a0, a1, a2}, {a0, a1, a2}] /.
  Table[δ[i] → (i - 3)  $\frac{\pi}{2}$ , {i, 1, numberSteps}]];

tanPhase = FullSimplify[ $\frac{-a2 /. ans[[1]]}{a1 /. ans[[1]]}$ ]

$$\frac{4 (\text{imeasured}[2] - 2 \text{imeasured}[4] + \text{imeasured}[6])}{-\text{imeasured}[1] + 7 \text{imeasured}[3] - 7 \text{imeasured}[5] + \text{imeasured}[7]}$$


```

As will be shown below, these algorithms are very insensitive to errors in the phase step.

## 6 Error Sources

---

There are many sources of errors in phase-shifting interferometry but the seven most common are

- 1) Incorrect phase shift between data frames,
- 2) Vibrations,
- 3) Detector non-linearity,
- 4) Stray reflections,
- 5) Quantization errors,
- 6) Frequency stability, and
- 7) Intensity fluctuations.

### 6.1 Error due to incorrect phase-shift between data frames

Incorrect phase shift between data frames can be due to many sources such as incorrect phase shifter calibration, vibration, or air turbulence. While the error in the phase shift could be non-linear due to errors such as vibration, a common error is simply a linear error. For example, the phase shift should be  $(n \frac{\pi}{2})$  and the actual phase shift is  $(n \frac{\pi}{2} + n \epsilon)$ .

The Plot Phase Error Module in Section 8.1 be used to determine errors due to a linear phase shift error. In this section we will look errors resulting incorrect phase shifts for several of the algorithms derived above. As our first example we will look at the errors associated with the four  $\frac{\pi}{2}$  step algorithm given in Equation 5.

#### 6.1.1 Four $\frac{\pi}{2}$ Steps

The first quantity sent to the plotPhaseError module is the numerator of the arctangent while the second quantity is the denominator of the arctangent. For the plotPhaseError module the measured irradiance values need to be called imeasured. The third quantity required is the number of steps, 4 in this case, and the next quantity is the phase step,  $\frac{\pi}{2}$ . The next quantity is the percent calibration error, which for our example we will set equal to 5. The next two quantities have to do with detector non-linearity, and for this example we will set equal to zero. The last three quantities have to do with the amplitude, frequency, and phase of the vibration, which for this example we will set equal to zero.

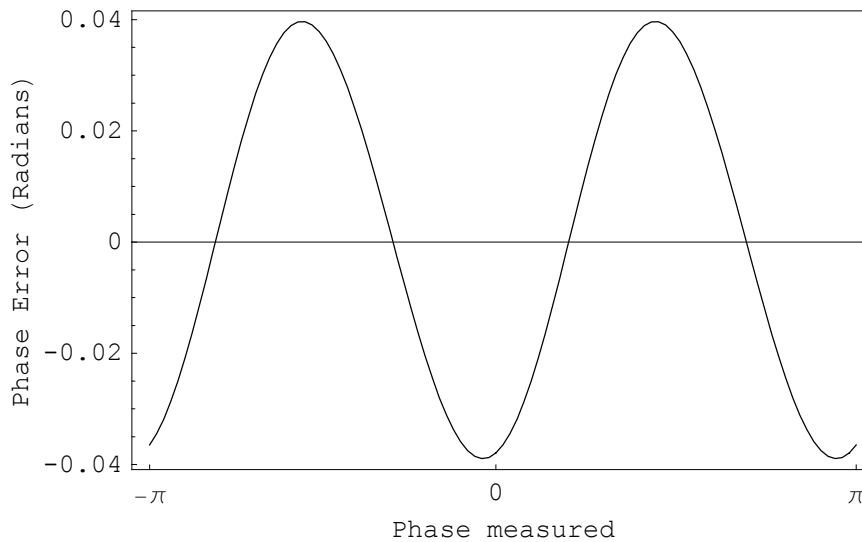
```

num = imeasured[4] - imeasured[2];
den = imeasured[1] - imeasured[3];
plotPhaseError[num, den, 4,  $\frac{\pi}{2}$ , 5, 0, 0, 0, 0, 0]

```

**Phase error due to 5% phase shift calibration error.**

Peak-Valley Error (Radians) = 0.0785302



The result shown above shows that for a 5% error in the calibration the peak-valley phase error is 0.0785 radians or 0.012 waves of OPD. This phase error is generally larger than what is acceptable, and this is the reason that generally more than four phase steps are used in the measurement. Of more importance than the number is the fact that the error is basically sinusoidal with a frequency equal to twice the frequency of the interference fringes. This turns out to be a very common result for phase calibration error.

### 6.1.2 Three $\frac{\pi}{2}$ Steps

Next we will look at the phase – shifting error for the three  $\frac{\pi}{2}$  step algorithm given in Equation 7.

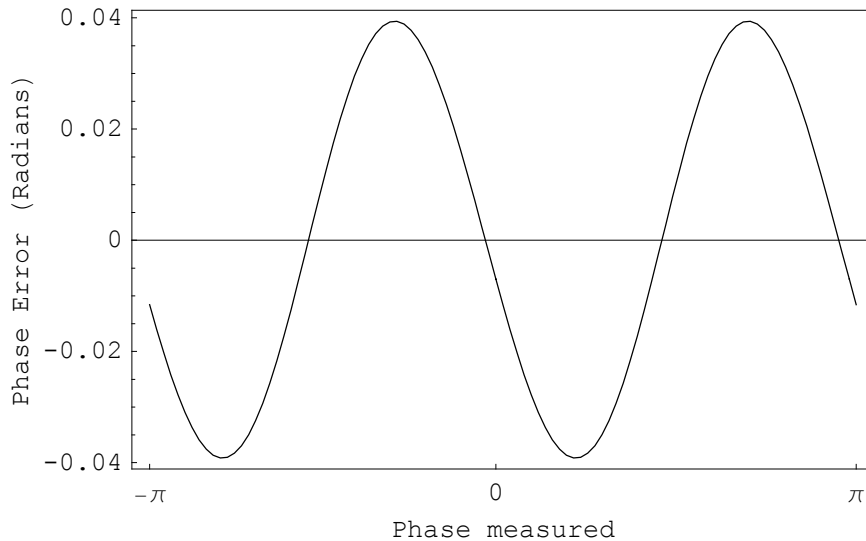
```

num = -(imeasured[2] - imeasured[3]);
den = imeasured[1] - imeasured[2];
plotPhaseError[num, den, 3,  $\frac{\pi}{2}$ , 5, 0, 0, 0, 0, 0]

```

**Phase error due to 5% phase shift calibration error.**

Peak-Valley Error (Radians) = 0.0785398



It is interesting that this is the same result we obtained using four  $\pi/2$  steps.

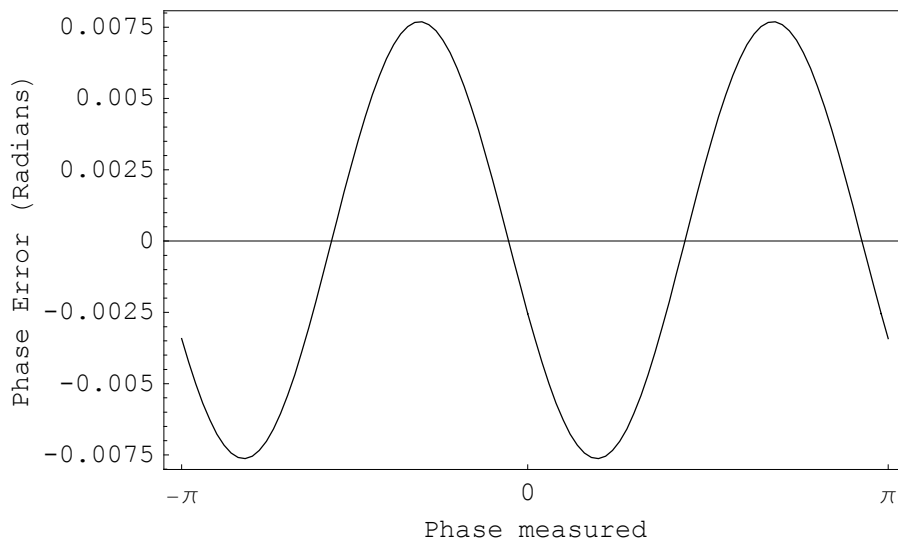
### 6.1.3 Five $\frac{\pi}{2}$ Steps

Next we will look at the phase-shifting error for the five  $\pi/2$  step algorithm given in Section 5.3.

```
num = 7 (imeasured[2] - imeasured[4]);
den =
- 4 imeasured[1] + imeasured[2] + 6 imeasured[3] + imeasured[4] - 4 imeasured[5];
plotPhaseError[num, den, 5,  $\frac{\pi}{2}$ , 5, 0, 0, 0, 0, 0]
```

**Phase error due to 5% phase shift calibration error.**

Peak-Valley Error (Radians) = 0.0153166



We see that by going from four steps to five steps we have reduced the peak-valley error by a factor of 5. However, we can do even better with five steps if we use the Schwider-Hariharan algorithm.

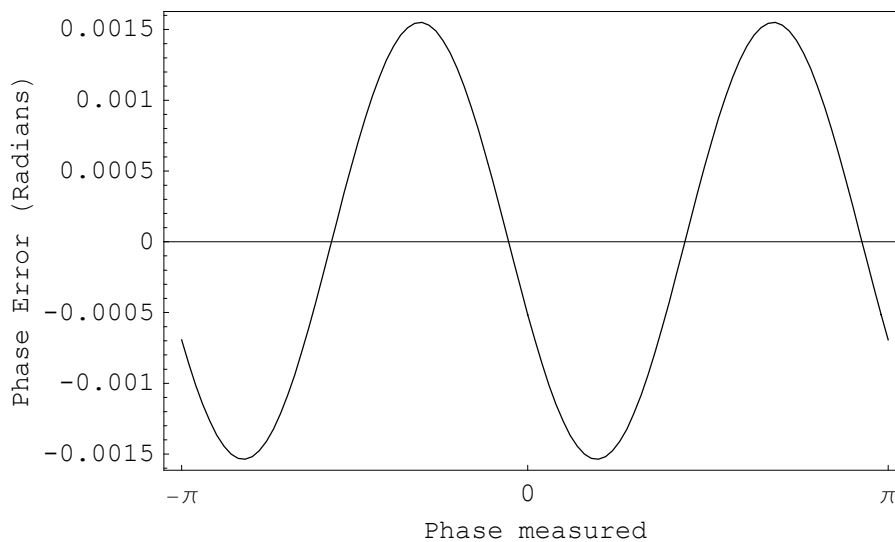
#### 6.1.4 Schwider-Hariharan Five $\frac{\pi}{2}$ Step Algorithm

We will now look at the phase-shifting error associated with the Schwider-Hariharan algorithm in Section 5.4.

```
num = -2 (imeasured[2] - imeasured[4]) ;
den = imeasured[1] - 2 imeasured[3] + imeasured[5] ;
plotPhaseError[num, den, 5,  $\frac{\pi}{2}$ , 5, 0, 0, 0, 0, 0]
```

**Phase error due to 5% phase shift calibration error.**

Peak-Valley Error (Radians) = 0.0030859



We have obtained another factor of 5 reduction in the peak-valley error, but we can do even better.

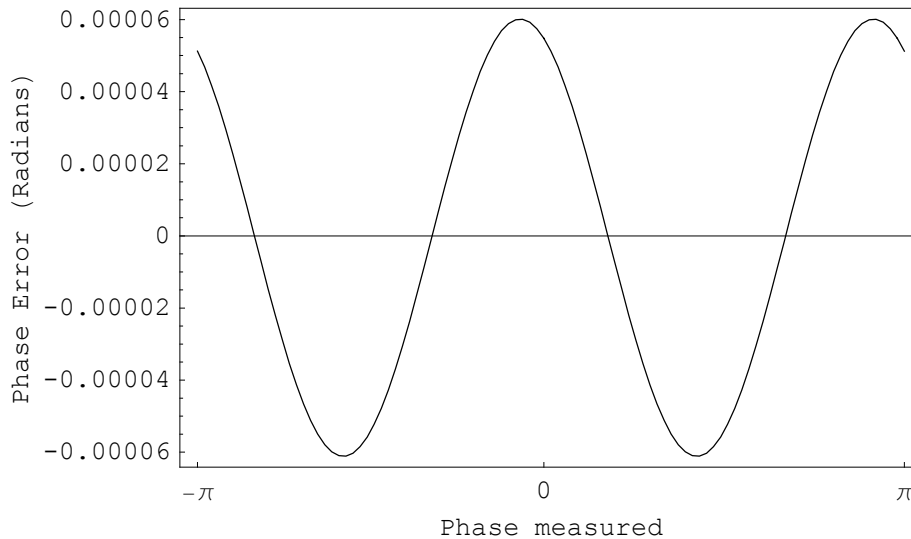
#### 6.1.5 Six $\frac{\pi}{2}$ Step Algorithm

We will now look at the phase-shifting error associated with the six  $\pi/2$  step algorithm in Section 5.5.

```
num = - (3 imeasured[2] - 4 imeasured[4] + imeasured[6]) ;
den = imeasured[1] - 4 imeasured[3] + 3 imeasured[5] ;
plotPhaseError[num, den, 6,  $\frac{\pi}{2}$ , 5, 0, 0, 0, 0, 0]
```

### Phase error due to 5% phase shift calibration error.

Peak-Valley Error (Radians) = 0.000121171



By going from 5 steps to 6 steps we have reduced the error due to a 5% incorrect phase shift by nearly a factor of 30.

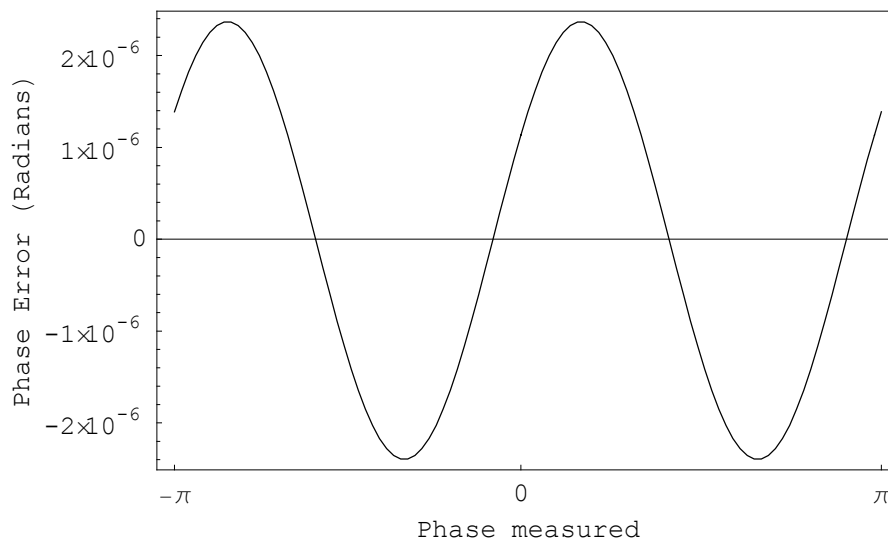
#### 6.1.6 Seven $\frac{\pi}{2}$ Step Algorithm

We will now look at the phase-shifting error associated with the seven  $\pi/2$  step algorithm in Section 5.5.

```
num = 4 (imeasured[2] - 2 imeasured[4] + imeasured[6]) ;
den = -imeasured[1] + 7 imeasured[3] - 7 imeasured[5] + imeasured[7] ;
plotPhaseError[num, den, 7,  $\frac{\pi}{2}$ , 5, 0, 0, 0, 0, 0]
```

### Phase error due to 5% phase shift calibration error.

Peak-Valley Error (Radians) = 0.00000475669



By going from 6 steps to 7 steps we have reduced the error due to a 5% incorrect phase shift by nearly another factor of 30. It is amazing, but by going from 5 steps to 7 steps we have reduced the error due to a 5% incorrect phase shift by nearly 3 orders of magnitude.

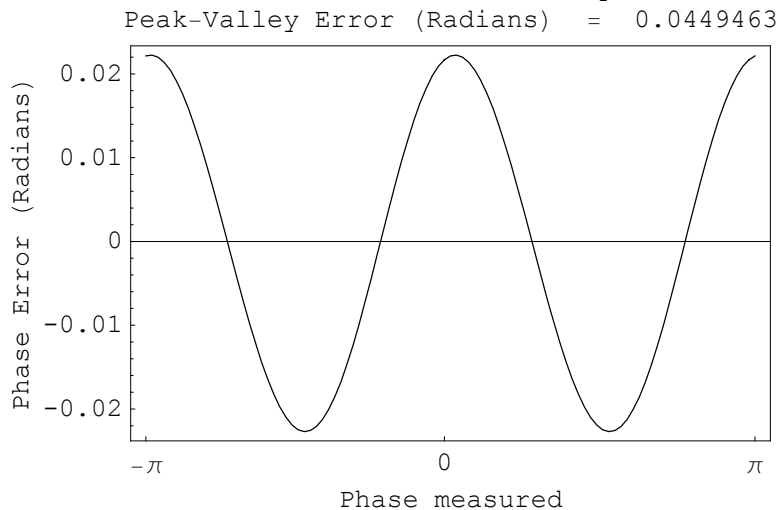
## 6.2 Error due to vibration

Probably the the most serious impediment to wider use of PSI is its sensitivity to external vibrations. The vibration sensitivity of PSI is a result of PSI using time-dependent phase shifts. Vibrations cause incorrect phase shifts between data frames. The errors are similar to those seen above, but they are much harder to correct because the optimum algorithm depends upon the frequency of the vibration present as well as the phase of the vibration relative to the phase shifting (Brophy 1990; de Groot and Deck 1996; Deck and de Groot 1998).

The Plot Phase Error Module can be used to see some of the effects of vibrations for phase-stepping. The last three variables sent to the module are  $\delta vib$ , the zero to peak amplitude of the vibration in units of wavelength;  $freq$ , the frequency of the vibration in units of the frame rate of the camera; and  $phaseVib$ , the phase of the vibration. The phase vibration is written as  $2 \pi \delta vib \sin[ freq 2 \pi i + phaseVib ]$ .  $i$  is equal to 1 for the first frame. The following shows one example for vibration of amplitude 0.1 wave and frequency equal to 0.3 times the frame rate, and vibration phase equal to  $\frac{\pi}{4}$ .

```
num = imeasured[4] - imeasured[2];
den = imeasured[1] - imeasured[3];
plotPhaseError[num, den, 4,  $\frac{\pi}{2}$ , 0, 0, 0, .02, .3,  $\frac{\pi}{4}$ ]
```

**Phase error due to 0.02 wave vibration  
amplitude having frequency 0.3 times  
frame rate and phase of  $\frac{\pi}{4}$ .**



It is not surprising that just as for phase shifter calibration error, the error due to vibration is at twice the fringe frequency.

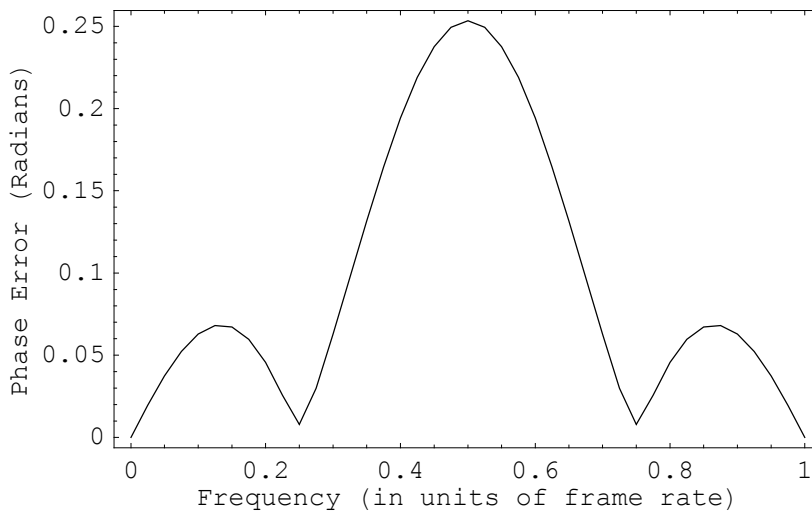
The vibration error module in Section 8.2 is used to determine the peak-valley of the error due to vibration. The plot vibration error module in Section 8.3 gives a plot of the peak-valley of the phase measurement error versus a frequency range of 0 to the frame rate of the camera for the phase-stepping mode of operation. The phase of the vibration is varied to determine the maximum peak-valley error.

The first quantity sent to the plot vibration error module is the numerator of the arctangent while the second quantity is the denominator of the arctangent. For the plotVibrationError module the measured irradiance values need to be called imeasured. The third quantity required is the number of steps, 4 for the first example, and the next quantity is the phase step, which for all examples will be  $\frac{\pi}{2}$ . The last quantity is the zero-peak amplitude of the vibration in units of wavelength. Due to the large number of calculations involved, the module takes a long time to complete the plot.

The following shows an example the four step step algorithm described above and a 1/50 wave vibration amplitude.

```
num = imeasured[4] - imeasured[2];
den = imeasured[1] - imeasured[3];
plotVibrationError[num, den, 4,  $\frac{\pi}{2}$ , 0.02];
```

### P-V phase error due to 0.02 zero to peak waves of vibration

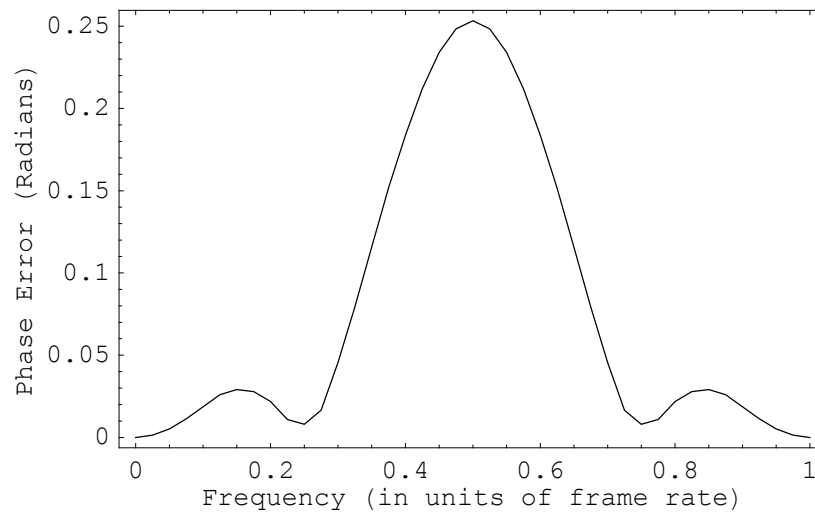


It should be noted that a 1/50 wave zero-peak (1/25 wave P-V) vibration amplitude produced a P-V phase error of 0.25 radians, which corresponds to a 1/25 wave. That is, the peak-valley error is equal to the peak-valley vibration amplitude and it occurs at a frequency of 1/2 the frame rate. For the most common frame rate of 30 frames/sec the most troublesome vibration frequency would be 15 Hz.

If we repeat the above for the Schwider-Hariharan five step algorithm we get the following:

```
num = -2 (imeasured[2] - imeasured[4]);
den = imeasured[1] - 2 imeasured[3] + imeasured[5];
plotVibrationError[num, den, 5,  $\frac{\pi}{2}$ , 0.02];
```

### P-V phase error due to 0.02 zero to peak waves of vibration



Note that the peak error at a frequency equal to one-half the frame rate is the same. The major change is that the secondary peaks are reduced.

## 6.3 Error due to detector non-linearity

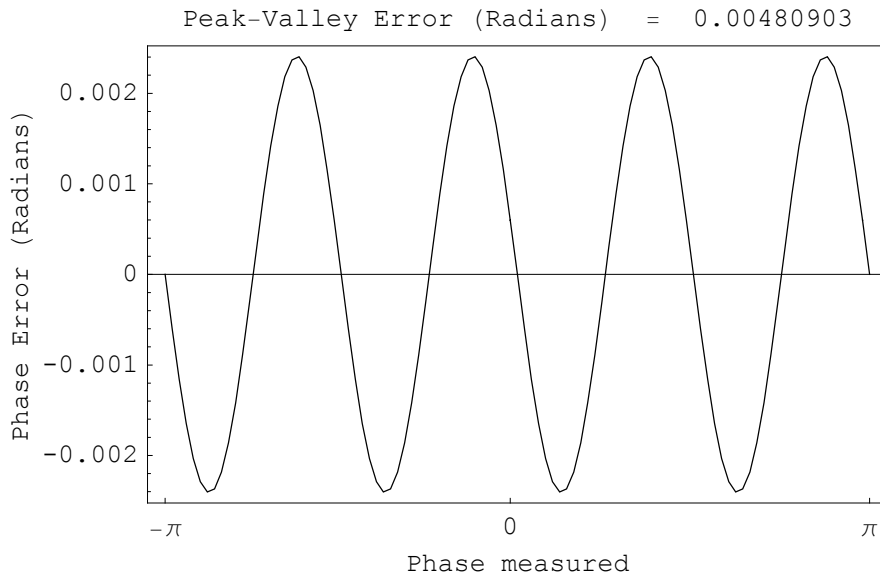
Generally CCDs have extremely linear response to irradiance, however sometimes the electronics between the detector and the digitizing electronics introduce some nonlinearity. The Plot Phase Error Module in Section 8.1 can be used to determine errors due to detector non-linearity. The quantities sent to the module are as described above with the addition of two quantities having to do with the detector non-linearity. The sixth quantity sent to the module is the percentage irradiance nonlinearity and the seventh quantity is the degree of non-linearity. For the examples below we set the non-linearity equal to 1 % for either order 2 or order 3.

### 6.3.1 Four $\frac{\pi}{2}$ Steps

As our first example we will look at the errors associated with the four  $\frac{\pi}{2}$  step algorithm given in Equation 5 and third-order detector nonlinearity.

```
num = imeasured[4] - imeasured[2];
den = imeasured[1] - imeasured[3];
plotPhaseError[num, den, 4,  $\frac{\pi}{2}$ , 0, 1, 3, 0, 0, 0]
```

### Phase error due to 1% detector nonlinearity of order 3.



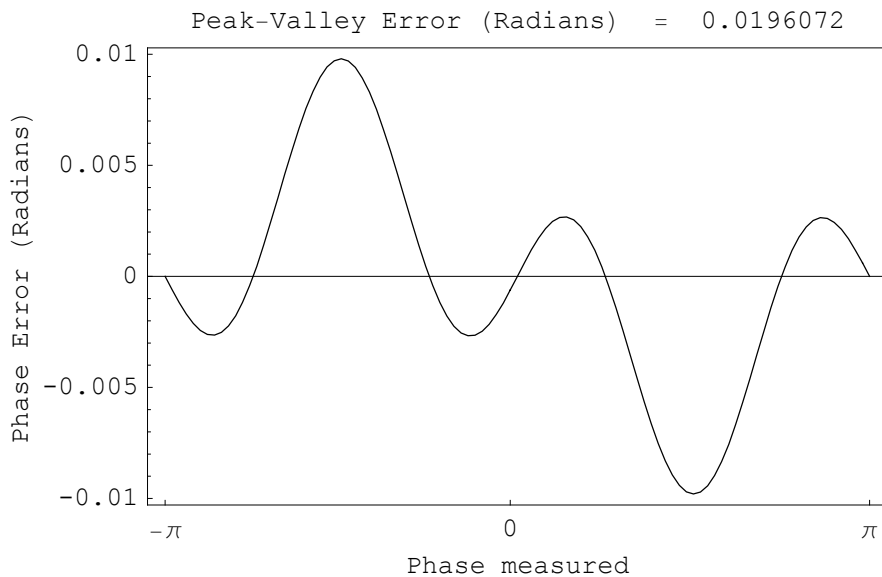
In this case the peak-valley error is 0.0048 radians and it is nearly sinusoidal with a frequency equal to 4 times the frequency of the interference fringes. The four times frequency is a common result for algorithms have  $\frac{\pi}{2}$  phase steps. If we had tried a quadratic detector non-linearity we would have found out there is no resulting phase error. This is an important result to remember.

#### 6.3.2 Three $\frac{\pi}{2}$ Steps

Next we will look at the detector nonlinearity error for the three  $\frac{\pi}{2}$  step algorithm given in Equation 7. In this case we will look at errors due to quadratic nonlinearity.

```
num = -(imeasured[2] - imeasured[3]);
den = imeasured[1] - imeasured[2];
plotPhaseError[num, den, 3,  $\frac{\pi}{2}$ , 0, 1, 2, 0, 0, 0]
```

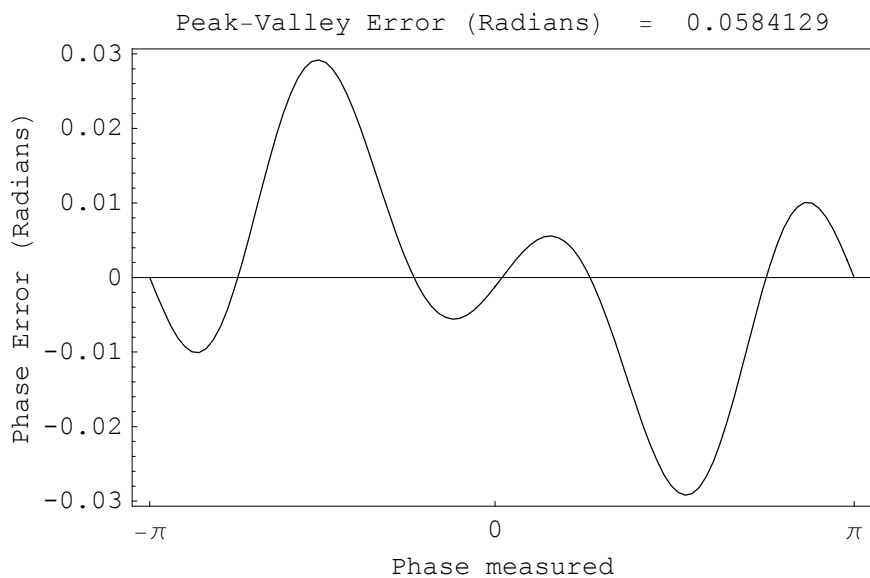
### Phase error due to 1% detector nonlinearity of order 2.



Next we will look at the error due to third-order detector nonlinearity.

```
num = -(imeasured[2] - imeasured[3]);
den = imeasured[1] - imeasured[2];
plotPhaseError[num, den, 3,  $\frac{\pi}{2}$ , 0, 1, 3, 0, 0, 0]
```

### Phase error due to 1% detector nonlinearity of order 3.



It is noted that the shape of the error is quite for three  $\pi/2$  steps than for four  $\pi/2$  steps. The error is quite bad.

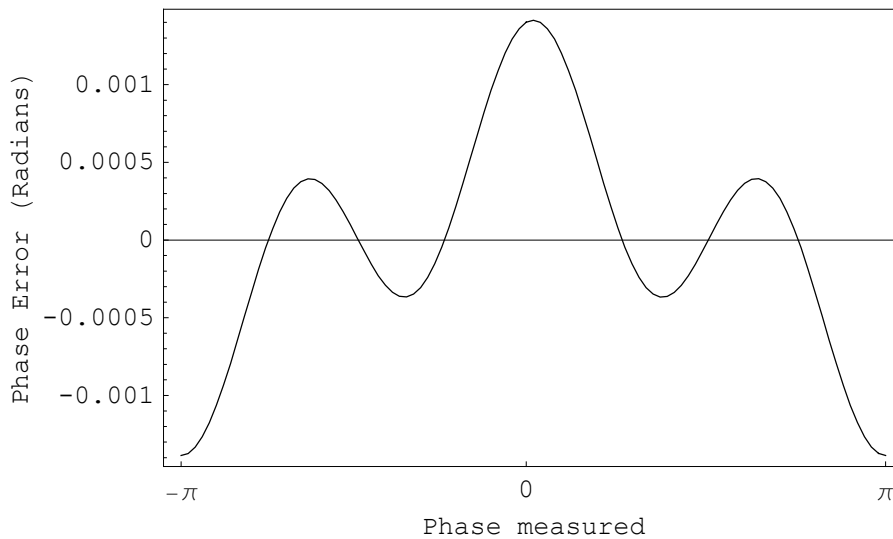
### 6.3.3 Five $\frac{\pi}{2}$ Steps

Next we will look at the detector nonlinearity error for the five  $\pi/2$  step algorithm given in Section 5.3. First we will look at second-order nonlinearity and then we will look at third-order detector nonlinearity effects.

```
num = 7 (imeasured[2] - imeasured[4]);
den =
  -4 imeasured[1] + imeasured[2] + 6 imeasured[3] + imeasured[4] - 4 imeasured[5];
plotPhaseError[num, den, 5,  $\frac{\pi}{2}$ , 0, 1, 2, 0, 0, 0]
```

**Phase error due to 1% detector nonlinearity  
of order 2.**

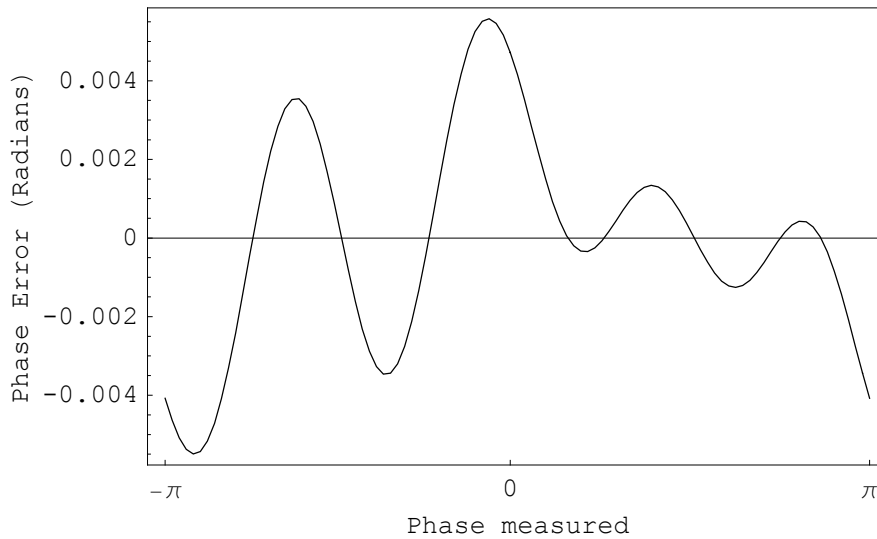
Peak-Valley Error (Radians) = 0.00280112



```
num = 7 (imeasured[2] - imeasured[4]);
den =
  -4 imeasured[1] + imeasured[2] + 6 imeasured[3] + imeasured[4] - 4 imeasured[5];
plotPhaseError[num, den, 5,  $\frac{\pi}{2}$ , 0, 1, 3, 0, 0, 0]
```

### Phase error due to 1% detector nonlinearity of order 3.

Peak-Valley Error (Radians) = 0.0110769



The errors have been reduced.

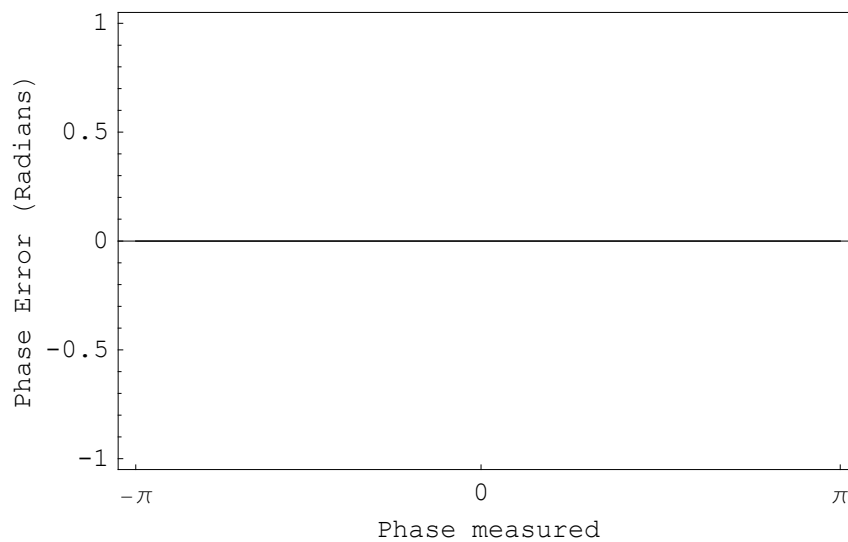
#### 6.3.4 Schwider-Hariharan Five $\frac{\pi}{2}$ Step Algorithm

We will now look at the phase-shifting error associated with the Schwider-Hariharan algorithm in Section 5.4.

```
num = -2 (imeasured[2] - imeasured[4]);
den = imeasured[1] - 2 imeasured[3] + imeasured[5];
plotPhaseError[num, den, 5,  $\frac{\pi}{2}$ , 0, 1, 2, 0, 0, 0]
```

### Phase error due to 1% detector nonlinearity of order 2.

Peak-Valley Error (Radians) = 0



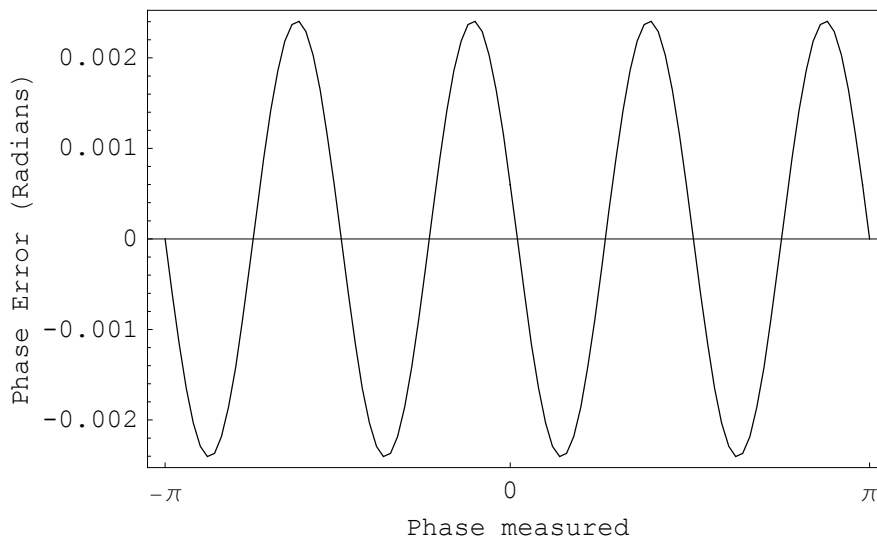
```

num = -2 (imeasured[2] - imeasured[4]) ;
den = imeasured[1] - 2 imeasured[3] + imeasured[5] ;
plotPhaseError[num, den, 5,  $\frac{\pi}{2}$ , 0, 1, 3, 0, 0, 0]

```

### Phase error due to 1% detector nonlinearity of order 3.

Peak-Valley Error (Radians) = 0.00480903



The error due to quadratic nonlinearity has been eliminated and the error due to third-order has been reduced by nearly a factor of 3. The Schwider-Hariharan algorithm is a very nice algorithm.

### 6.3.5 Six $\frac{\pi}{2}$ Step Algorithm

We will now look at the phase-shifting error associated with the six  $\pi/2$  step algorithm in Section 5.5.

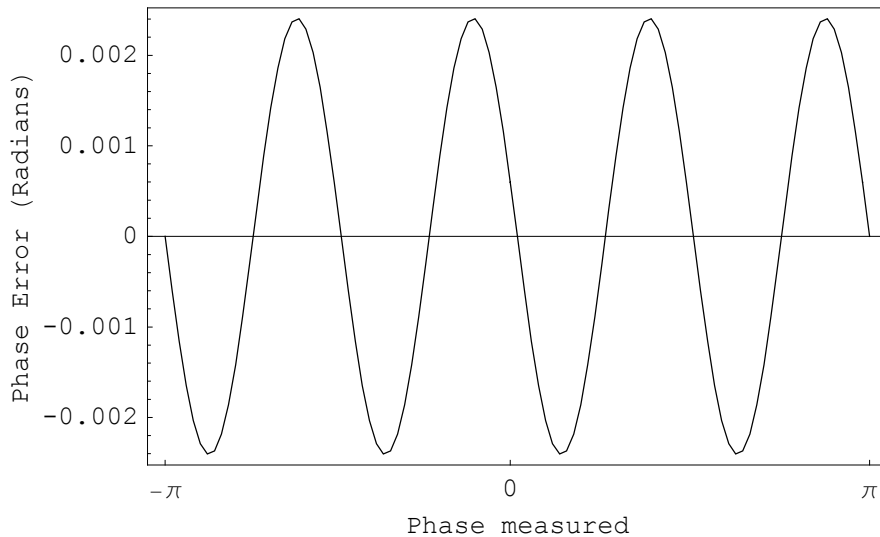
```

num = -(3 imeasured[2] - 4 imeasured[4] + imeasured[6]) ;
den = imeasured[1] - 4 imeasured[3] + 3 imeasured[5] ;
plotPhaseError[num, den, 6,  $\frac{\pi}{2}$ , 0, 1, 3, 0, 0, 0]

```

### Phase error due to 1% detector nonlinearity of order 3.

Peak-Valley Error (Radians) = 0.00480903



Although we do not show it the error due to quadratic nonlinearity is again zero, and the interested result is that the error due to third-order is the same for 6 steps as it was for 5 steps.

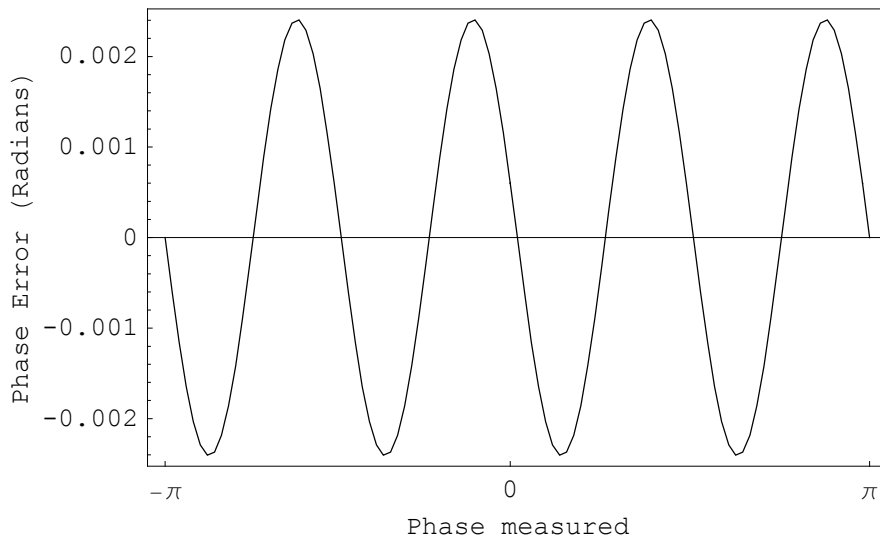
#### 6.3.6 Seven $\frac{\pi}{2}$ Step Algorithm

We will now look at the phase-shifting error associated with the seven  $\pi/2$  step algorithm in Section 5.5.

```
num = 4 (imeasured[2] - 2 imeasured[4] + imeasured[6]) ;
den = -imeasured[1] + 7 imeasured[3] - 7 imeasured[5] + imeasured[7] ;
plotPhaseError[num, den, 7,  $\frac{\pi}{2}$ , 0, 1, 3, 0, 0, 0]
```

### Phase error due to 1% detector nonlinearity of order 3.

Peak-Valley Error (Radians) = 0.00480903



Although we do not show it the error due to quadratic nonlinearity is again zero, and the interesting result is that the error due to third-order is the same for 7 steps as it was for 5 and 6 steps.

## 6.4 Error due to stray reflections

A common problem in interferometers using lasers as a light source is extraneous interference fringes due to stray reflections. The easiest way of thinking about the effect of stray reflections is that the stray reflection adds to the test beam to give a new beam of some amplitude and phase. The difference between this resulting phase, and the phase of the test beam, gives the phase error. If we express the amplitude of the stray light as a fraction of the amplitude of the test beam we can write

$$\text{amplitudeMeasured} = E^{i\text{phaseTest}} + \text{amplitudeStray} E^{i\text{phaseStray}};$$

As an example let

$$\text{phaseTest} = 30 \text{ Degree}; \quad \text{phaseStray} = 90 \text{ Degree}; \quad \text{amplitudeStray} = \frac{1}{5};$$

Then

$$\text{phaseMeasured} = N[\text{ArcTan}[\text{Re}[\text{amplitudeMeasured}], \text{Im}[\text{amplitudeMeasured}]]]$$

0.679776

The error in the measurement in degrees is given by

$$\text{phaseError} = (\text{phaseMeasured} - \text{phaseTest}) / \text{Degree}$$

8.94828

If the stray light is not changed by blocking the test beam, the phase and amplitude of the stray light can be measured, and the effect of the stray light on the phase measurement can be determined. However, often the stray light changes if the test beam is blocked. In well designed laser based interferometers the stray light is minimal. Probably the best way of reducing or eliminating the error due to stray light is to use a short coherence light source.

## 6.5 Quantization error

The first step in getting irradiance information into the computer is to digitize the detector output. The digitization should be done in the electronics as close to the camera as possible, and in the best situations it is done within the camera. Generally 8 bits (256 levels) are used in the digitization, but sometimes 10 bits (1024 levels) or 12 bits (4096 levels) or more are used. If the fringe modulation does not span the full dynamic range of quantization levels the effective number of bits is less than the quantization level.

Brophy (Brophy 1990) has shown that the standard deviation of the phase error due to b bit digitization for an n step algorithm goes as

$$\sigma_{\phi} [n_, b_] := \frac{2}{\sqrt{3 n} 2^b};$$

The standard deviation of the calculated phase in units of wavelengths as a function of the number of bits and the number of steps in the algorithm is given in the table below.

```

error = TableForm[N[Table[ $\frac{\sigma_\phi[n, b]}{2 \pi}$ , {b, 8, 12}, {n, 4, 7}], 3],
  TableHeadings -> {"8 bits", "9 bits", "10 bits", "11 bits", "12 bits"},
  {"4-step", "5-step", "6-step", "7-step"}]

```

	4-step	5-step	6-step	7-step
8 bits	0.000359	0.000321	0.000293	0.000271
9 bits	0.000179	0.000161	0.000147	0.000136
10 bits	0.0000897	0.0000803	0.0000733	0.0000678
11 bits	0.0000449	0.0000401	0.0000366	0.0000339
12 bits	0.0000224	0.0000201	0.0000183	0.000017

As the table indicates, 8 bits is generally sufficient, but sometimes 10 or 12 are required. It is important to point out again that if the fringe digitization does not span the full dynamic range of quantization the effective number of bits is less than the quantization level. Also, if the noise is greater than one bit, quantization error can be reduced by averaging data sets.

## 6.6 Frequency stability error

If the source frequency changes and the paths are not matched a phase shift will be introduced between the two interfering beams. If  $d$  is the path difference,  $c$  is the velocity of light, the phase difference,  $\Delta\phi$ , introduced by a frequency difference,  $\Delta\nu$ , is given by

$$\Delta\phi = 2\pi \frac{d}{c} \Delta\nu;$$

While frequency changes will introduces errors in the phase shifting, as described by many authors for example (Tatsuno and Tsunoda 1987; Ishii et al. 1987; Wizinowich, 1990), the phase shifting can be produced by a frequency shift.

## 6.7 Intensity fluctuations error

If intensity fluctuations of the source introduce errors in the measured phase. It has been shown (Bruning 1978; Koliopoulos 1981) that source intensity fluctuations cause the standard deviation in the measured wavefront phase to go as

$$\sigma_\phi = \frac{1}{\sqrt{n s}};$$

where  $n$  is the number of phase steps and  $s$  is the signal-to-noise.

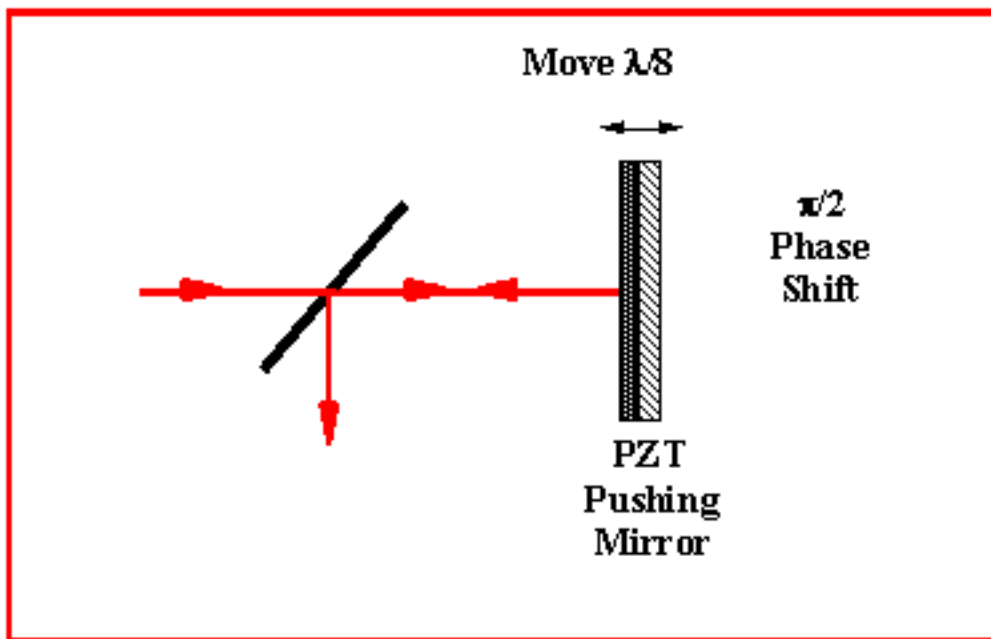
In the ideal situation the noise limitation is set by photon shot noise (Wyant 1975). If  $p$  is the number of detected photons, the standard deviation of the measured wavefront phase goes as

$$\sigma_\phi = \frac{1}{\sqrt{p}};$$

## 7 Phase Shifters

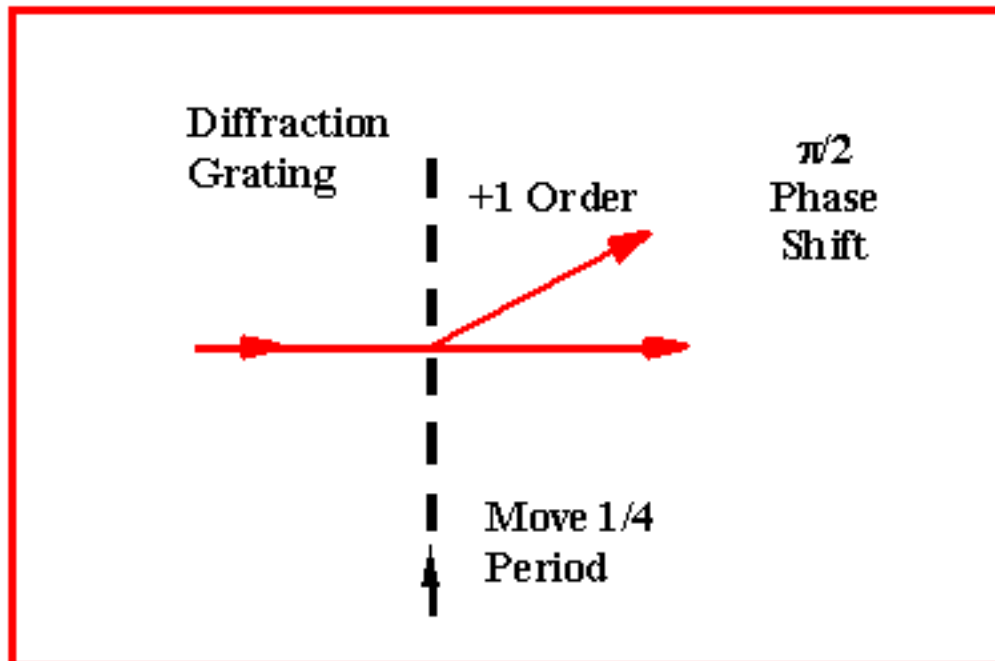
### 7.1 Moving Mirror

The most common method for phase shifting is to reflect one of the two interfering beams off a moving mirror. If the light is incident upon the mirror at an angle of  $\theta$ , and the mirror moves a distance  $d$ , the phase is shifted by an amount equal to  $\frac{2\pi}{\lambda} 2 d \cos[\theta]$ . At normal incidence the phase shift is  $\frac{2\pi}{\lambda} 2 d$ . Thus, for a  $\pi/2$  phase shift the mirror must be moved  $1/8$  wavelength. A piezoelectric transducer (PZT) is the most common way of translating the mirror. The position of the mirror is controlled by the voltage applied to the PZT.



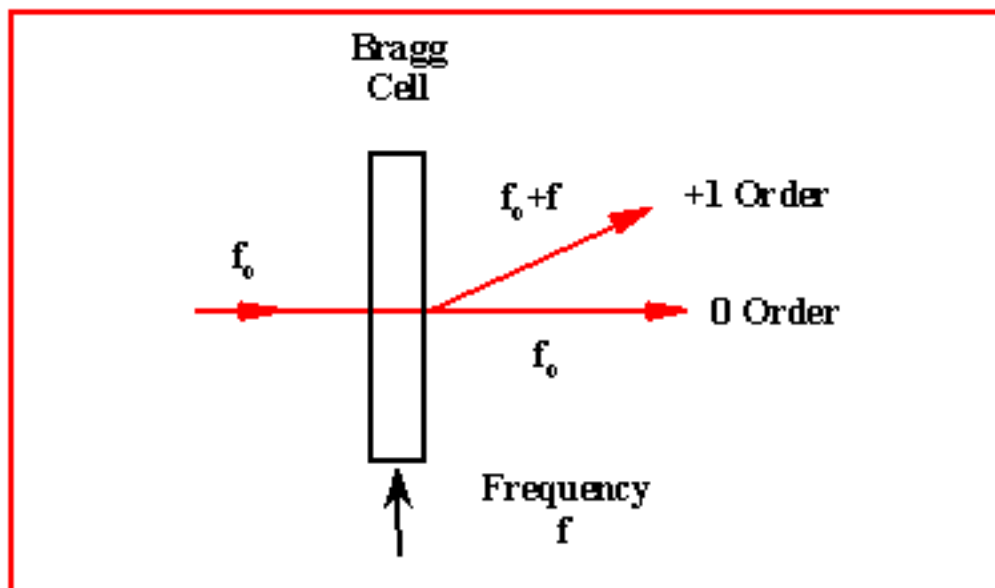
### 7.2 Moving Diffraction Grating

A moving grating is another good way of changing the phase difference between two interfering beams. It can be shown that as a grating is moved one grating spacing the  $n$ th diffraction order is phase shifted an amount  $n 2\pi$ . Thus, if a grating is translated  $1/4$  period the phase of the first order is changed  $\pi/2$ . The phase of the minus first order is changed  $-\pi/2$ .



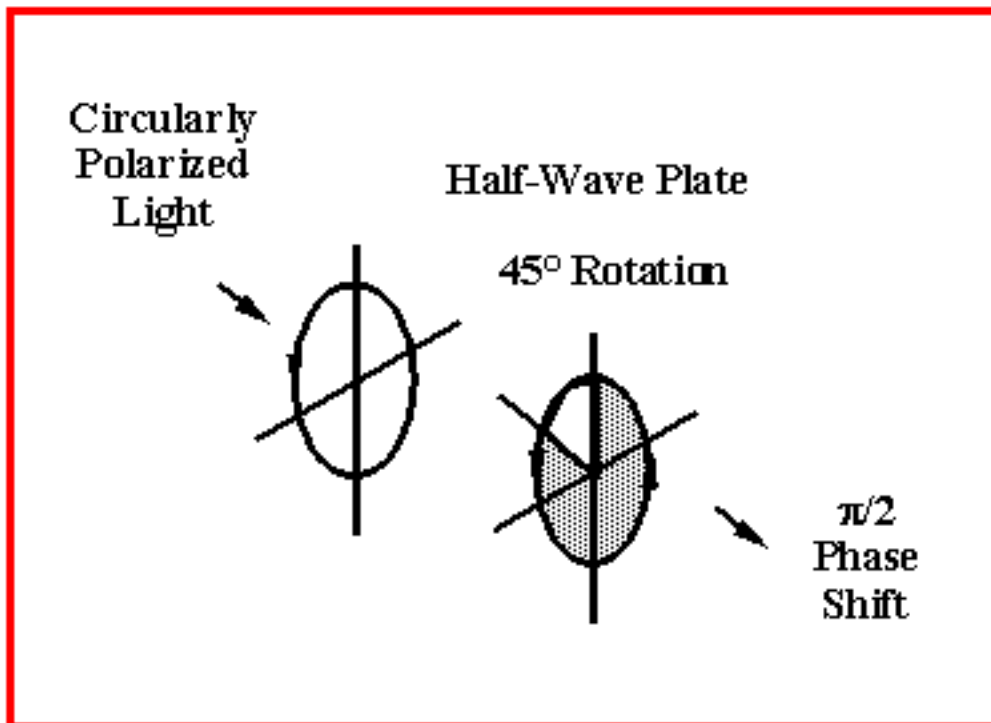
### 7.3 AO Bragg Cell

An acousto optic Bragg cell can be thought of as a moving grating. If the Bragg cell is driven with an electrical frequency,  $f$ , the first order is frequency shifted an amount  $f$ . Bragg cells are very useful in phase-shifting systems where the phase is changed at a constant rate. The frequency shift is very constant and the signal is very clean.



## 7.4 Rotating Half-Wave Plate

There are several polarization techniques useful for phase shifting. One example is shown below. If a circularly polarized beam of light is transmitted through a half-wave plate the sense of polarization will be changed, i.e. left-handed to right-handed and vice-versa. It can be shown that if the half-wave plate is rotated an angle  $\theta$ , the phase of the light is shifted an amount  $2\theta$  (Shagam and Wyant 1978).



## 7.5 Phase Shifter Calibration

An important part of operating a phase-shifting interferometer is the calibration of the phase shifter. With most commercial PSI systems this is now automated.

One method for performing the calibration is to use the solution for  $\alpha$  in the Carré algorithm in Section 4.2. Note that the phase shift is  $2\alpha$ . However, there are many other equations that can be used for the calibration. A simpler and more commonly used phase shifter calibration algorithm is one using the first two frames and the last two frames of a five-frame measurement (Cheng and Wyant 1985). The following is a simple way of both understanding this algorithm and observe its limitation.

Let the irradiance be given by

$$i = a_0 + a_1 \cos[\delta] + a_2 \sin[\delta];$$

Let there be 5 phase shift increments where the phase step is  $\alpha$ .

$$\delta = \{-2\alpha, -\alpha, 0, \alpha, 2\alpha\};$$

Then the irradiances of the five steps are

$$i \{ a_0 + a_1 \cos[2\alpha] - a_2 \sin[2\alpha], a_0 + a_1 \cos[\alpha] - a_2 \sin[\alpha], \\ a_0 + a_1, a_0 + a_1 \cos[\alpha] + a_2 \sin[\alpha], a_0 + a_1 \cos[2\alpha] + a_2 \sin[2\alpha] \}$$

Subtracting the first from the fifth yields

$$i[[5]] - i[[1]] \\ 2 a_2 \sin[2\alpha]$$

Subtracting the second from the fourth yields

$$i[[4]] - i[[2]] \\ 2 a_2 \sin[\alpha]$$

Therefore,

$$\text{Simplify} \left[ \frac{1}{2} \frac{i[[5]] - i[[1]]}{i[[4]] - i[[2]]} \right] \\ \cos[\alpha]$$

That is,

$$\alpha = \text{ArcCos} \left[ \frac{1}{2} \frac{i[[5]] - i[[1]]}{i[[4]] - i[[2]]} \right]$$

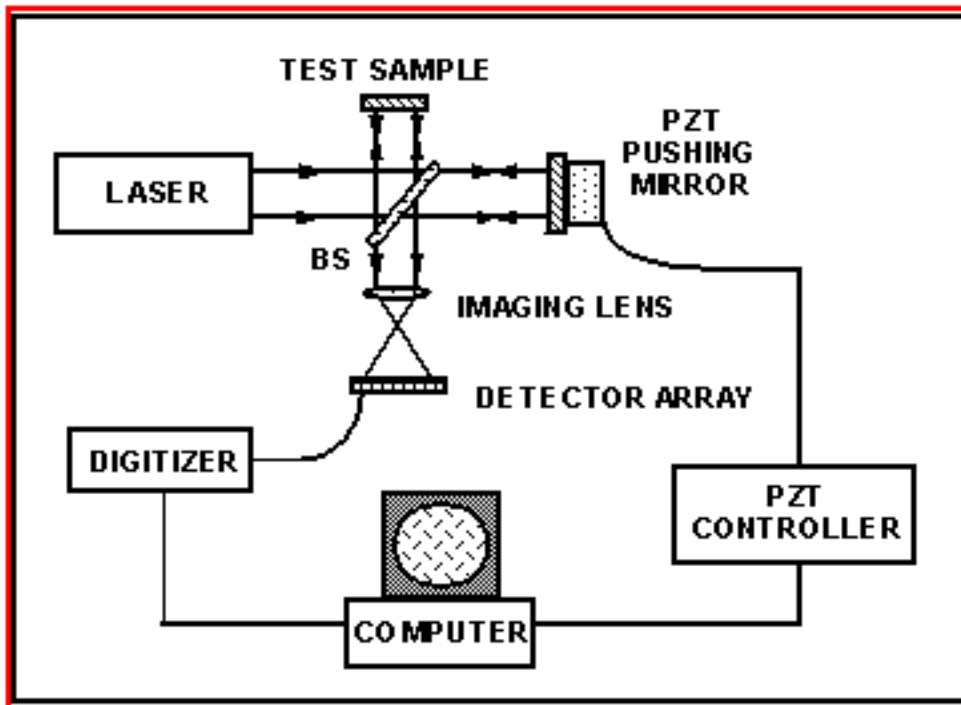
The third frame is not used. Generally we want  $\alpha$  to be  $\pi/2$ . The sign of  $i[[5]] - i[[1]]$  tells us whether  $\alpha$  is too large or too small.

A limitation of this algorithm (as well as the Carré algorithm) is that there are singularities for certain values of the wavefront phase. In this example there is a singularity when  $a_2$  is equal to zero. Remember that  $a_2$  is proportional to the sine of the phase. To avoid errors, a few tilt fringes are introduced into the interferogram and data points for which  $i[[5]] - i[[1]]$  or  $i[[4]] - i[[2]]$  are smaller than a threshold are eliminated.

It is often convenient to look at a histogram of the phase shifts. If the histogram is wider than some preselected value it is known that there must be problems with the system such as too much vibration present. The standard deviation of the phase shifts is an excellent way of identifying problems with the phase shifting.

## 7.6 Phase-Shifting Interferometer

The figure below illustrates a phase-shifting Twyman-Green interferometer. In this case the phase shifter is a moving mirror mounted on a PZT. The computer reads out a digitized signal from a detector array as it controls the voltage applied to the PZT.



## 8 Software Modules

---

## 9 References

---

Ai, C. and J. C. Wyant, "Effect of Spurious Reflection on Phase Shift Interferometry," *Appl. Opt.*, 27, 3039 (1988).

Angel, J. R. P. and P. L. Wizinowich, "A Method of Phase Shifting in the Presence of Vibration," *European Southern Observatory Conf. Proc.*, 30, 561 (1988).

Brophy, C. P., "Effect of Intensity Error Correlation on the Computed Phase of Phase-Shifting Interferometry," *J. Opt. Soc. Am. A*, 7, 537 (1990).

Bruning, J. H., D. R. Herriott, J. E. Gallagher, D. P. Rosenfeld, A. D. White, and D. J. Brangaccio, "Digital Wavefront Measuring Interferometer for Testing Optical Surfaces and Lenses," *Appl. Opt.*, 13, 2693 (1974).

Bruning, J. H., "Fringe Scanning Interferometers," in *Optical Shop Testing*, D. Malacara, Ed., Wiley, New York, 1978.

Carré, P. "Installation et Utilisation du Comparateur Photoelectrique et Interferentiel du Bureau International des Poids de Mesures," *Metrologia* 2, 13 (1966).

Cheng, Y.-Y. and J. C. Wyant, "Phase Shifter Calibration in Phase-Shifting Interferometry," *Appl. Opt.*, 24, 3049 (1985).

Crane, R., "Interference Phase Measurement," *Appl. Opt.*, 8, 538 (1969).

---

Creath, K., "Phase-Measurement Interferometry Techniques," in Progress in Optics. Vol. XXVI, E. Wolf, Ed., Elsevier Science Publishers, Amsterdam, 1988, pp, 349- 393.

de Groot, P., "Derivation of algorithms for phase-shifting interferometry using the concept of a data-sampling window," Appl. Opt., 34, 4723 (1995).

de Groot, P. and L. Deck, "Numerical simulations of vibration in phase-shifting interferometry," Appl. Opt., 35, 2172 (1996).

Deck, L. and P. de Groot, "Punctuated quadrature phase-shifting interferometry," Opt. Lett., 23, 19 (1998).

Freischlad, K. and C. L. Koliopoulos, "Fourier description of digital phase-measuring interferometry," J. Opt. Soc. Am. A, 7, 542 (1990).

Greivenkamp, J.E. and J. H. Bruning, "Phase Shifting Interferometers," in Optical Shop Testing, D. Malacara, Ed., Wiley, New York, 1992, pp, 501-598.

Greivenkamp, J. E., "Generalized Data Reduction for Heterodyne Interferometry," Opt. Eng., 23, 350 (1984).

Hardy J., J. Feinleib, and J. C. Wyant, "Real time phase correction of optical imaging systems," OSA Topical Meeting on Opt. Propagation through Turbulence, Boulder, Colorado, July 1974.

Hariharan, P., B. F. Oreb, and T. Eiju, "Digital Phase-Shifting Interferometry: A Simple Error-Compensating Phase Calculation Algorithm," Appl. Opt., 26, 2504 (1987).

Ishii, Y., J. Chen, and K. Murata, "Digital Phase-Measuring Interferometry with a Tunable Laser Diode," Opt. Lett., 12, 233 (1987).

Koliopoulos, C. L., "Interferometric Optical Phase Measurement," Ph.D. Dissertation, Univ. Arizona, Tucson, 1981.

Morgan, C. J., "Least-Squares Estimation in Phase-Measurement Interferometry," Opt. Lett., 7, 368 (1982).

Phillion, D. W., "General methods for generating phase-shifting interferometry algorithms," Appl. Opt. 36, 8098 (1997).

Schmit, J. and K. Creath, "Extended averaging technique for derivation of error-compensating algorithms in phase-shifting interferometry," Appl. Opt., 34, 3610 (1995).

Shagam, R. N. and J. C. Wyant, "Optical Frequency Shifter for Heterodyne Interferometers Using Simple Rotating Polarization Retarders," Appl. Opt., 17, 3034 (1978).

Schwider, J., R. Burow, K. E. Elssner, J. Grzanna, R. Spolaczyk, and K. Merkel, "Digital Wavefront Measuring Interferometry: Some Systematic Error Sources," Appl. Opt., 22, 3421 (1983).

Tatsuno, K. and Y. Tsunoda, "Diode Laser Direct Modulation Heterodyne Interferometer," Appl. Opt., 26, 37 (1987).

Wizinowich, P. L., "Phase-Shifting Interferometry in the Presence of Vibration: A New Algorithm and System," Appl. Opt., 29, 3271 (1990).

Wyant, J. C., "Use of an ac Heterodyne Lateral Shear Interferometer with Real-Time Wavefront Correction Systems," Appl. Opt., 14, 2622 (1975).

Wyant, J. C., C. L. Koliopoulos, B. Bhushan and O. B. George, "An Optical Profilometer for Surface Characterization of Magnetic Media," ASLE Trans., 27, 101 (1984).